ELECTRICITY

FROM

PHOTOVOLTAICS

BY: SABRI M. SHERIF

2002-03

Department of Mechanical

Engineering

Faculty of Engineering

University of Strathclyde

THE COPYRIGHT

ACKNOWLEDGEMENTS

I owe gratitude to Dr Craig Mclean who undertook the supervision of this project. I would like to thank him for his enthusiasm, his guidance and for sharing his wide experience with me.

I would also like to thank MR Cameron Johnstone for giving freely of his time for little reward and for his guidance and instruction in doing the experiment and with out him which this thesis would not have reached completion.

I would like to thank Mr Eric Duncan for his co-operation and help doing the preparation of laboratory items.

I would also like to thank all the postgraduate students at Strathclyde University.

I would especially like to thank my wife and my children for them support.

I would like to record my gratitude to Libya embassy especially for Mr Younes Almahdi whose student supervisor for financial support through out the course.

ABSTRACT

The aim of this project is to show how to produce the electricity from photovoltaic solar cells and there are experiment proofing that and overview of techniques and principles of cell design. Although there is excellent example where a lot of the concepts discussed in one design the PERL design for high-efficiency Silicon Si solar cells. These techniques and principles are the result of intensive research over the last forty years that has required the simultaneous understanding of electrical and optical effects. The remaining challenge is to find accost-effective way to apply these principles to construct a low-cost solar cell with high and stable efficiency.

Photovoltaic (PV) cells have social and commercial value only when they are used in a system to provide a service. This research has given a brief overview of the technical and economic considerations that allow the cells to provide such a service.

: CONTENTS:

CHAPTER 3

CHAPTER 4

CHAPTER 5

CHAPTER one

INTRODUTION

1-INTRODUTION

Due to the limited reserves of both fossil and nuclear fuels, renewable resources will have to play major role in the world’s future energy supply.

Among potential new energy sources are solar energy and especially the Photovoltaic cells which generate electric power when illuminated by sunlight or artificial light. They are by far the most highly developed of the man-made photoconversion devices. Born of the space age in the 1950s, their earliest terrestrial applications emerged in the 1970s and they are now poised for significant market expansion in the new millennium.

Photovoltaic technology has a number of advantages over conventional methods of electricity generation. First, solar energy is the world’s major renewable energy resource. Photovoltaic power can be generated from the sun any where in temperate or tropical locations and in urban or rural environments. As a fuel-free distributed resource, photovoltaics could, in long run, make a major contribution to national energy security and carbon dioxide abatement. Photovoltaic is uniquely scalable, the only energy source that can supply power on a scale of milliwatts to megawatts from an easily replicated modular technology with excellent economies of scale in manufacture. Typical crystalline silicon Photovoltaic cell generates about 1.5 peak watts[1] (W_P) of direct current (DC) power, a typical Photovoltaic module about 50 W_P and the world’s largest multimodule arrays generate upward of a megawatt apiece. Photovoltaic cells are made of thin films. They contain small amounts of non-toxic materials and when manufactured in volume, have modest embedded energy. They posses no moving parts, they don’t need cooling water system and they are silent in operation. Photovoltaic systems are easy to use and long-live if properly maintained.

Photovoltaic has three drawbacks.

1- The intermittence and seasonality of sunlight.

2- Photovoltaic systems are very costly.

3- Photovoltaic is one faced by many emergent technologies-ignorance.

CHAPTER two

PRINCIPLES OF CELL DESIGN

2-PRINCIPLES OF CELL DESIGN

2.1- Main cell types

First one single-junction homo-and heterostructure solar cells where p-n homojunction is the most straightforward realisation of solar cell and the dominance of Silicon homojunction solar cells is a testimony to the success of this approach. But the single junction cell will never provide the highest conversion efficiency because of the trade-off between current and voltage.

Second one multijunction system where a cell fabricated in a semiconductor with a low band gap will provide a larger current because of its good light absorption over a broader spectral region. However it will never produce high open-circuit voltages because the open-circuit voltage can never exceed the band gap of the material. In practice the open-circuit voltage is limited by the large dark currents in a low-band-gap material.

Third one metal-semiconductor junctions (Schottky diode) with rectifying properties would also be suitable for the construction of a solar cell. But from the point of view of ease of production this approach suffers from limitations caused by the high dark currents flowing in such structures as compared to the heterojunction approach. In addition the predicted efficiency of solar cells based on metal-semiconductor junctions will be below 10% (see e.g.Hovel, 1975).

The last one is the metal-insulator-semiconductor (MIS) solar cell which the efficiencies above 20% (see Metz, 1997) and efficiencies as high as 23% are predicted (Kuhlmann, 1997) for a MIS-inversion layer cell.

2.2- optical design of cells

2.2.1- Light trapping

A lambertian surface is one that scatters light uniformly in all [forward] directions and lambertian light-trapping schemes are based on full internal randomisation of the light ray direction by a lambertian surface. Two possible implementations are shown in (Fig.2.1 (a, b)).

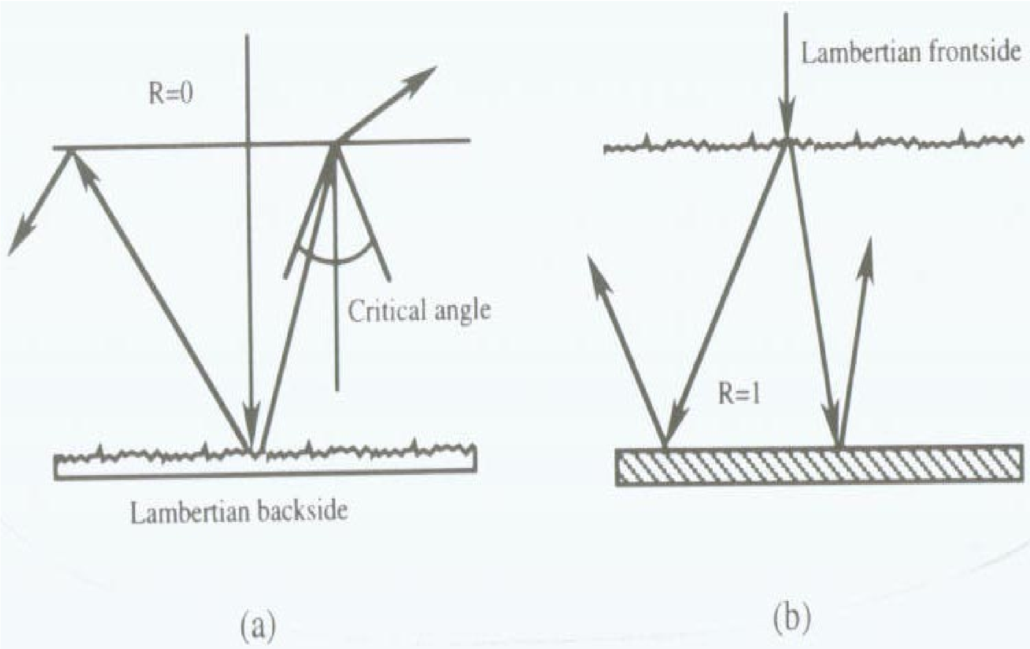

Figure (2.1) (a) Schematic of a cell with a perfect lambertian rear reflector and front surface with zero reflectance; (b) schematic of a cell with a perfect specular rear reflector and a lambertian front surface.

Light-trapping structures with lambertian surfaces represent the limiting case for cells with an isotropic response, i.e. cells whose response is independent of the angle of incidence (Tiedje, 1984). Because of the directionality of sunlight the use of surface structures with dimensions larger than the wavelength of the light can increase the cell absorptions above the limits of the lambertian schemes.

Additional improvement in light-trapping behaviour is obtained by structuring the backside of the cell. A very efficient method is use of backside grooves perpendicular to the frontside grooves as shown in Fig.2.2a. In Fig.2.2b a recently proposed concept with structuring of both sides is shown (Jorgensen et al., 1997). This structure gives rise to a further improvement of light-trapping properties.

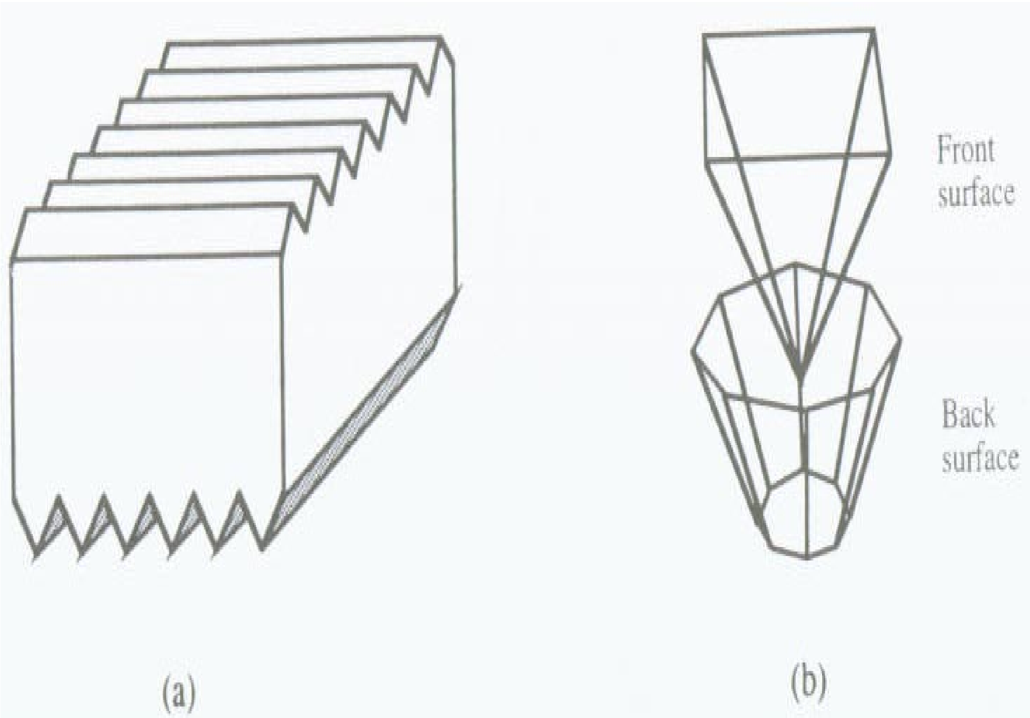

Figure (2.2) (a) Artist’s view of a cell with light-trapping structures at both front- and backside. The grooves at the frontside are perpendicular to the grooves at the backside (after Green, 1995, p.104, reproduced with permission from The Centre for Photovoltaic Devices and Systems); (b) structure, proposed by Jorgensen, 1997, reproduced with permission from IEEE.)

2.2.2- anti-reflective coatings: reduction of first reflection

The reduction of the front-surface reflectance is achieved by the use of so-called anti-reflective coatings (ARC). The ARC layer which is interposed between the photovoltaic cell material and the surrounding environment acts as a quarter-wavelength impedance matching element between the characteristic impedance of the environment and the photovoltaic material.

2.3- Design and fabrication of the metal contacts

The section will address the design of the metallization scheme. First one the design of the most widespread two-sided contacting scheme. The second one is one-sided contacting scheme.

2.3.1- Two-sided contact design

Optimisation of the front contact pattern

Most designs of the cells are based on two-sided contacting scheme, a schematic illustration of which is shown in Fig.2.3a and b. Fig.2.3b shows a cross-section of the two-dimensional contacting scheme. Although the carrier flow inside the cell is mostly vertical, the flow in the upper (emitter) layer of the cell is in the horizontal direction towards the collecting fingers.

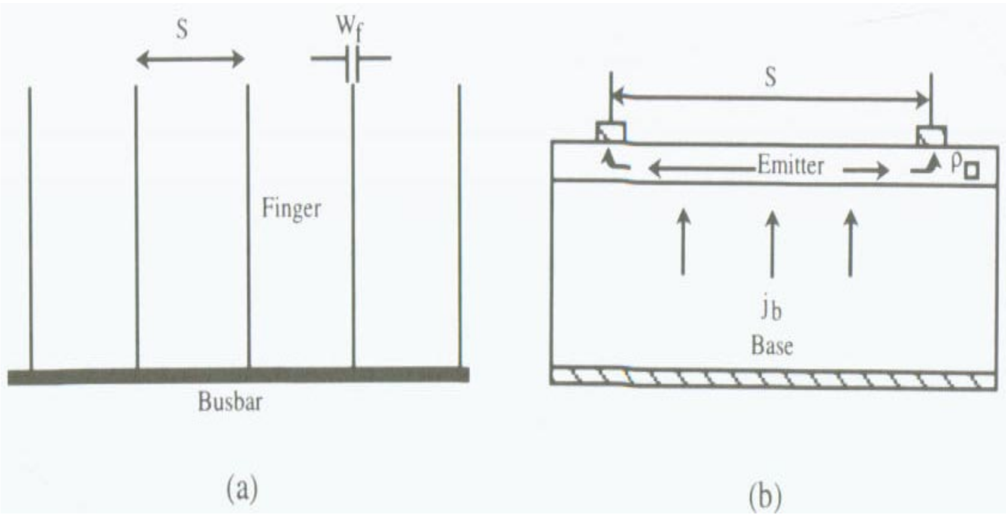

Figure (2.3) (a) Typical front contact lay-out. S is the finger spacing and Wf is the finger width. In the simple case, the finger width is constant; (b) cross section of cell showing the vertical carrier flow in the base of the cell and the horizontal majority carrier flow in the emitter.

The main design parameters are those relating to the finger grid at the frontside of the cell: the finger spacing S and the finger width W_f. Detailed optimisations based on the real two-dimensional carrier flow inside silicon (Si) high-efficiency n^+-p Si homojunction cell can be found in the work of Aberle, 1994.

When the carrier flux j_b towards the junction is homogeneously distributed and the upper layer is characterised by the sheet resistance ρ_{sheet}, the resistive losses in the upper layer per unit length of finger are given by

$$\int_0^{S/2} I^2 (x)\, dR = \int_0^{S/2} j^2_b\, b^2\, x^2\, \rho_{sheet}\, dx$$

$$= j^2_b\, S^3 \rho_{sheet}/8$$

This value compared with the maximum power delivered by the cell:

$$P_{mp} = V_{mp}\, I_{mp}\, S/2$$

Where V_{mp} and I_{mp} are the current and voltage generated at the maximum power point.

Then the relative loss defined as the ratio of the contact loss to the maximum power is given by

$$\text{Relative loss} = \rho_{sheet}\, I_{mp}\, S^2/4V_{max}$$

This equation shows the importance of the finger spacing and the sheet resistance of the upper layer. Achieving low values for the sheet resistance is obviously a promising way to reduce the resistive losses. Decreasing this by going to deeper emitters or thicker transparent conductive layers will increase other losses.

Screen printing

This technique widely is used for industrial non-concentrating silicon Si solar cells and the main advantage of screen printing is simplicity and cost-effectiveness. Drawbacks which are often cited are the relatively large line width, the high contact resistance due to oxide precipitation from the glass frit (dispersed glass particles), and the low (broad and flat) aspect ratio of the metal lines, which results in large shadowing losses. As a result, efficiencies between 17% and 17.5%, both on large-area monocrystalline (Nijs et al., 1996) and industrial-type multicrystalline (Shirasawa et al., 1994) Si cells have been reported.

Plating/buried contact technology

Plating is technique whereby a metal, dissolved in an aqueous solution, is deposited on a substrate. This can be realised by passing a direct current through the solution (electroplating), but in the context of Si solar cells the most widely used technique is electroless plating. Here the plating is performed by chemical deposition under such circumstances that the metal deposition occurs selectively in regions where the Si surface is in direct contact with the solution.

The low aspect ratio of the contacts is one of the drawbacks of the screen-printing technique. A solution to this problem is the so-called ‘buried contact’ technology, whereby the metal is electrolessly plated into deep grooves, obtained by laser scribing or mechanical cutting. A cross section of the final cell is shown in Fig 2.4.

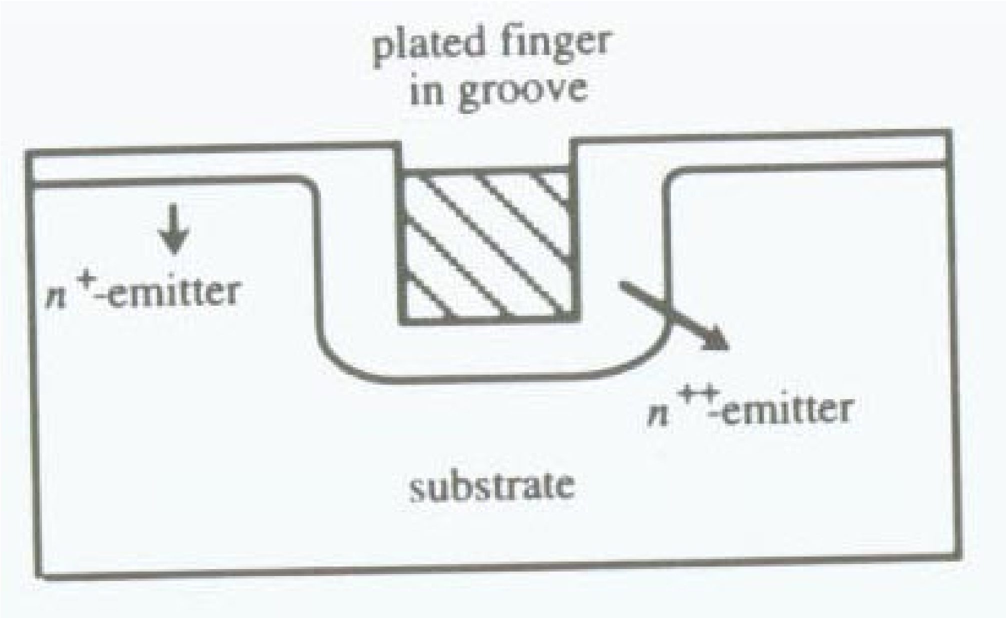

Figure (2.4) Schematic cross section of buried-contact structure.

The first versions of this technology made use of an oxide layer in between the grooves to avoid metal deposition (see e.g. Wenham, 1993). Subsequently this oxide layer was replaced by a nitride layer since this withstands high temperature steps and also provides better anti-reflection properties. The buried-contact approach is inherently a selective emitter approach, because two different diffusions are carried out during the process. There is a shallow diffusion in between the grooves, but a very deep diffusion within the grooves. Together with the low shadowing losses resulting from the high aspect ratio of the fingers, this technology has produced efficiencies between 16% and 18% on mono- and multicrystalline large-area Si solar cells.

Transparent conductive oxides

When the sheet resistance of the emitter is high the use of a finger contact pattern at the frontside of the cell is excluded. Under such circumstances a high-conductance layer covering the front surface is necessary. The transparent conductive oxides (TCOs) are a special class of materials that exhibit good electrical conductive high optical transparency and a high band gap. This makes them especially useful as n-type ‘window layers’ or transport layers on top of the actual window layer.

2.3.2- One-sided contact designs

One-sided contact designs are of very strong interest. An obvious advantage is the elimination of shadowing losses when all the contacts are at the backside. This is important in cells for concentrating systems where shadowing losses are more important. Additionally one-sided contact designs are particularly attractive at the level of module production. Monolithic integration of cells on a large insulating substrate could be an important factor in cost reduction because the series interconnection between the front contacts of a cell to the backside of the next cell in a conventional module forms an important part of module production costs.

Cell structures with all contacts at backside

We can distinguish two versions of his cell type, the point-contact and interdigitated designs shown in (Fig. 2.5 (a, b)). The main difference between the two is the reduced backside area with a high doping and metallization in the point-contact design which achieves higher open-circuit voltages because of reduced recombination at the surfaces.

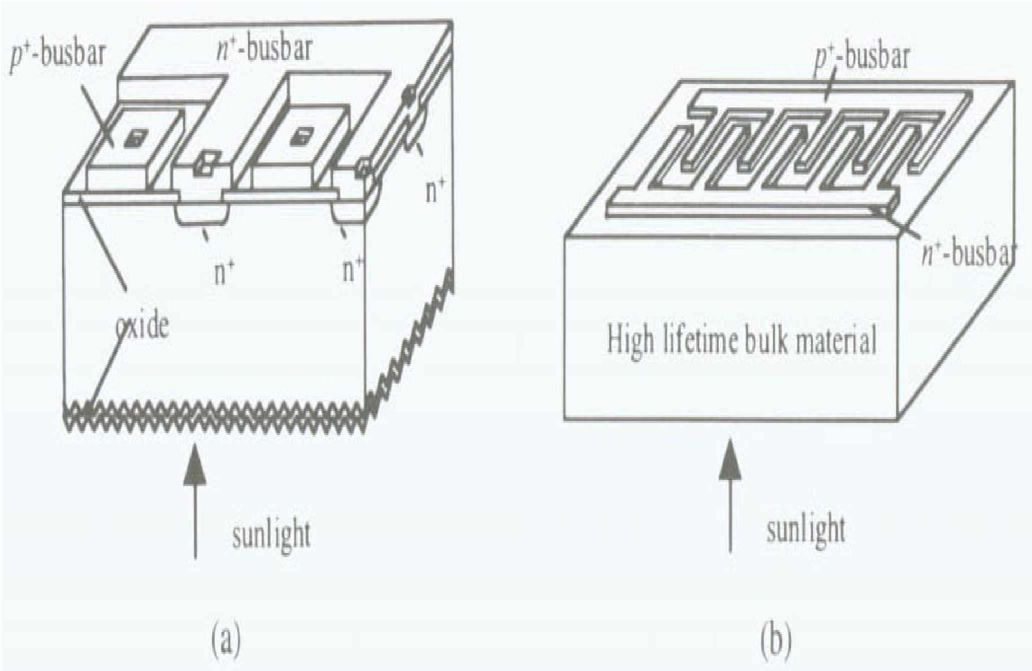

Figure (2.5) (a) backside point-contacted solar; (b) backside interdigitated solar cell.

Cell structures with all contacts at frontside

Although the advantage of no shadowing loss is lost if all the contacts are at the frontside, several groups like (Hebling 1995) are working on this concept in the context of developing a thin-film crystalline Si solar cell technology on an insulating substrate see (Fig 2.6).

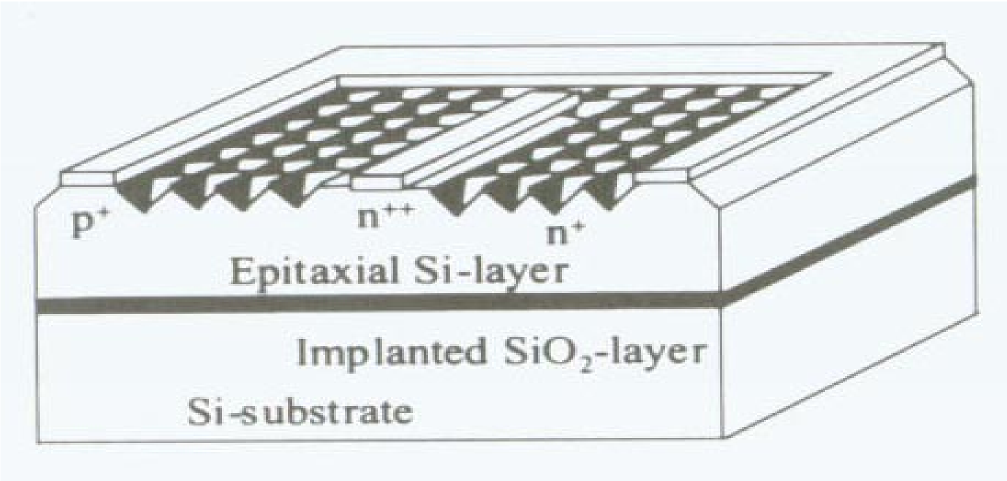

Figure (2.6) Frontside-contacted interdigitated cell (after hebling, 1995).

CHAPTER three

CYSTALLINE SILICON SOLAR CELLS

3-CYSTALLINE SILICON SOLAR CELLS

3.1-Overview

The majority of solar cells fabricated to date have been based on silicon in monocrystalline or large-grained polycrystalline form.

There are two main reasons for this. The first reason is that silicon is an elemental semiconductor with good stability and a well-balanced set of electronic, physical and chemical properties, the same set of strengths that have made silicon the preferred material for microelectronics. The second reason why silicon cells have been so dominant is that the success of silicon in microelectronics has created an enormous industry where the economies of scale directly benefit the presently smaller photovoltaics industry.

Most silicon cells have been fabricated using thin wafers cut from large cylindrical monocrystalline ingots prepared by the exacting Czochralski (CZ) crystal growth process and doped to one part per million with boron during ingot growth.

To produce a cell, these boron-doped starting wafers generally have phosphorus diffused at high temperatures a fraction of a micron into the surface to form the p-n junction required. Each cell is typically 10-15 cm either in diameter or along either side if square or rectangular.

Cells are sold interconnected and packaged into a weatherproof, glass-faced package known as a module, as in (Fig. 3.1.) since each cell gives a maximum output of about 0.6 volts in sunlight. This meaning we get over 20 voltages in one module because in each module there are 36 cells soldered together in series.

The efficiency of the cells in the module would typically lie in the 12-16% range, less than half the fundamental ‘detailed-balance’ limits of 33% for silicon (Tiedje 1984). Module efficiency is slightly lower than that of the constituent cells due to the area lost by frames and gaps between cells, with module efficiency generally lying in the 10-13% range. Over the last few years, commercial cells and modules of significantly higher performance have been available in multi-megawatt quantities using a more advanced cell processing technology. This technology produces cells of 17-18% efficiency and module efficiency in the 14-15% range.

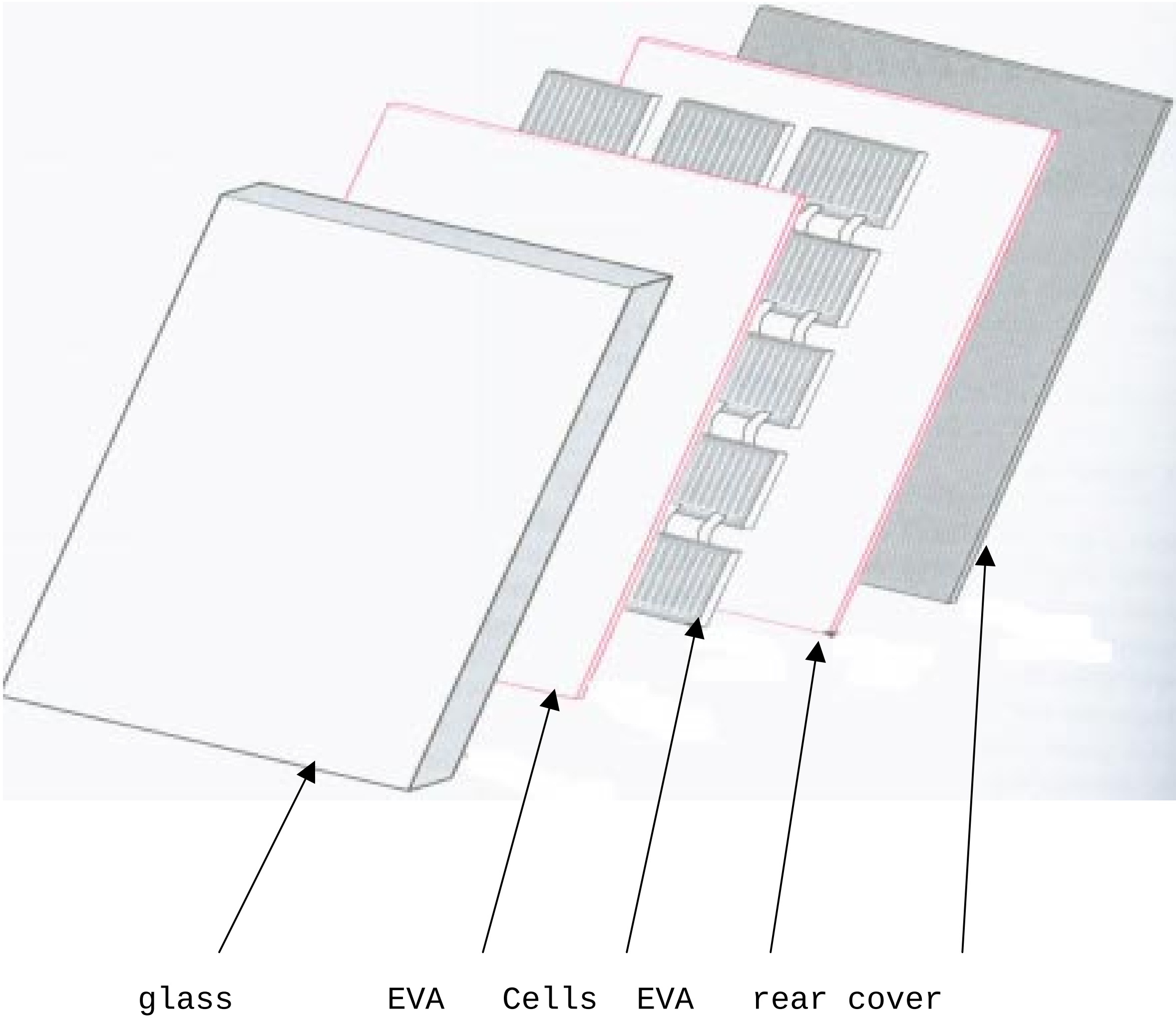

Figure (3.1) Exploded view of a standard silicon photovoltaic module. These layers laminated together under pressure at a temperature around 140-150 C where the transparent EVA (ethylene vinyl acetate) softens and binds the different layers together on cooling. Source: Green and Hansen (1998).

3.2-Silicon cell development

The development of silicon photovoltaics is inextricably intertwined with the development of the general silicon electronics field and the subsequent founding of the microelectronics industry. The rapid increase in interest in the properties of doped silicon led directly to the development of point contact and junction transistors and junction transistors and ultimately to integrate circuits.

The improvements of the early 1970s came about primarily by improving the ability of the cell to collect carriers generated by the incoming photons. Since cells now appeared to be performing to close to their full potential in this area, it seemed that any further improvement in silicon cell performance would have to result from improved open-circuit voltage. (Brandhorst and Bbernatowicz, 1980).

The successful approach has been the simplification of the ingot growth processes by using cruder directional solidification or casting approaches to produce multicrystalline ingots (Ferazza, 1996). These multicrystalline approaches involve basically a reversion to the earlier ingot-forming approaches for crystal rectifiers, techniques predating the microelectronics explosion. In this time the multicrystalline silicon cells accounted for about 30% of the total market for photovoltaic product. Another major area of developmental emphasis has been to reduce the thickness of the silicon wafer by slicing it more thinly.

The University of New South Wales developed microgroove PESC (passivated emitter solar cell) (FIG.3.2a) which was the first silicon cell to exceed 20% energy conversion efficiency in 1985. Other groups have used the same basic as roach to produce cells of similar efficiency, with commercial quantities produced for solar car racing and space. The approach is characterised by the use of a thin thermally grown oxide to ‘passivate’ (reduce the electronic activity of) the top surface of the junction diffusion (he emitter of the cell), combined with the use of a shallow, high sheet resistivity phoshorus diffusion for this emitter. Another is the use of photolithography to produce relatively small contact area to this emitter region by defining openings in the ‘passivated oxide’.

Cells of a similar quality to the first 20% efficient PESC have also found heir way into high-volume terrestrial cell manufacture through the laser-grooved buried-contact cell of (FIG.3.2b). The buried-contact approach now produces the highest performance terrestrial cells that are produced in any appreciable volume; with efficiency in the 17-18% range routinely obtained using Standard low-cost commercial silicon wafers.

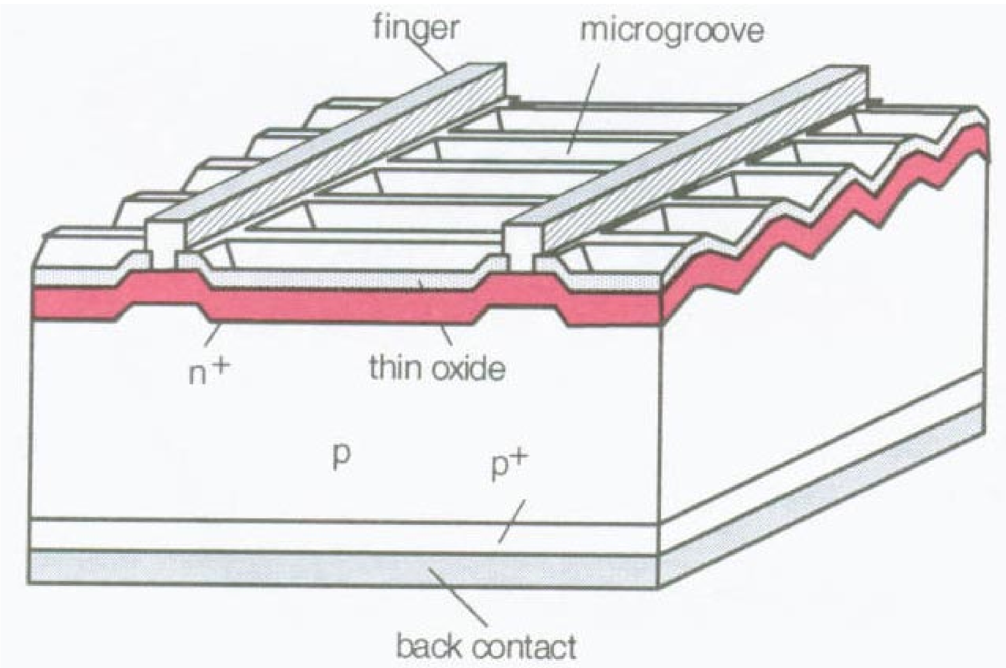

(a)

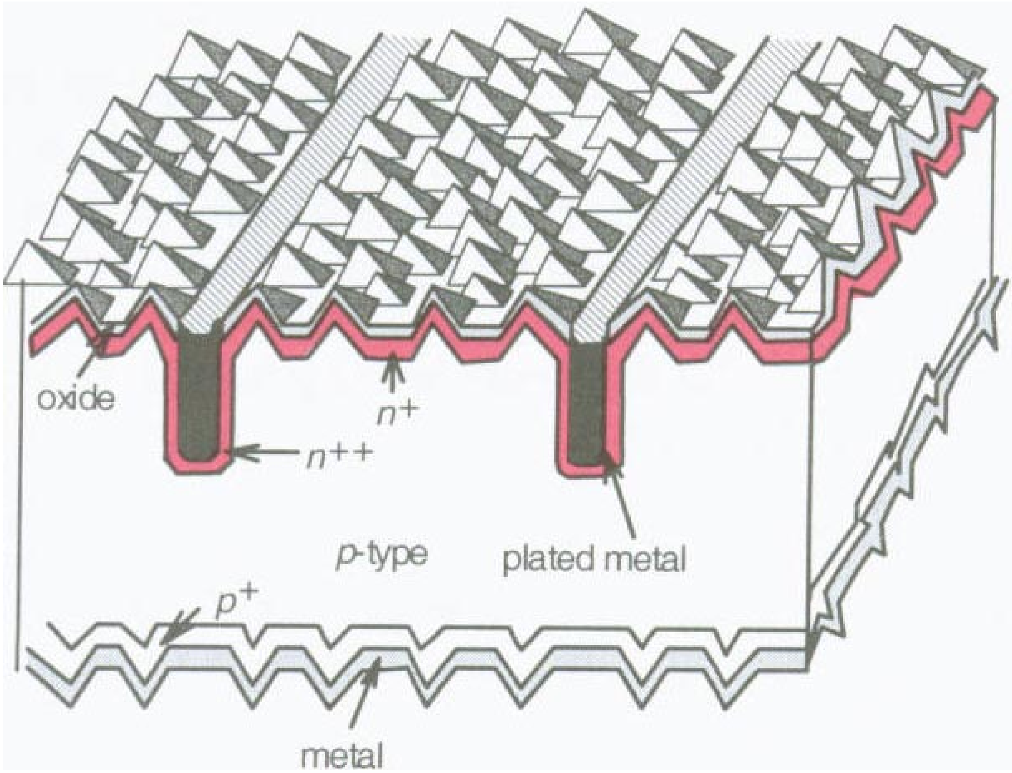

(b)

Figure (3.2) (a) The microgrooved passivated emitter solar cell (PESC cell) of 1985, the first silicon cell to exceed 20% efficiency; (b) buried-contact solar cell. Source: Green (1995).

The next improvement in silicon cell design came in the use of oxide passivation along both the front and rear surfaces, as first demonstrated in the rear point contact solar cell developed by Stanford University. As shown in (FIG.3.3), this cell has an unusual design in hat both positive and negative contacts are made at the rear surface of the cell. The rear point contact cell demonstrated 22% efficiency in 1988 and has since been commercialised, finding use in photovoltaic systems which rely on concentrated sunlight and for high value-added applications such as solar car racing and high-altitude aircraft flights (Verlinden et al.,1997).

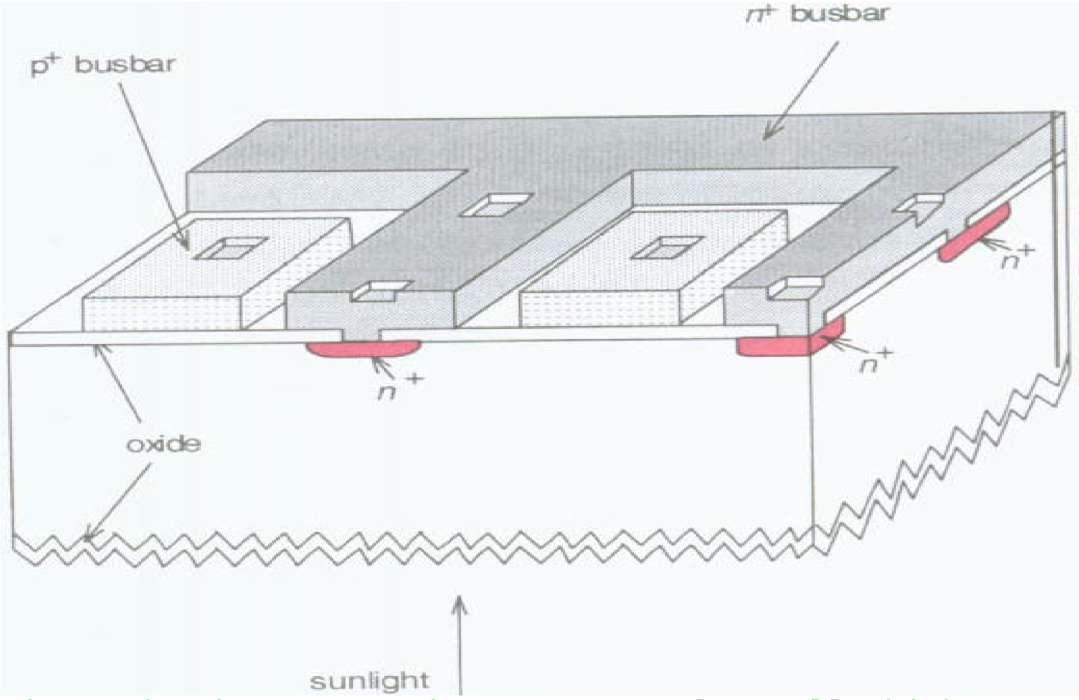

Figure (3.3) Rear point contact solar cell which demonstrated 22% efficiency in 1988 (cell rear shown uppermost). Source: Green (1995).

The next improvement in silicon cell efficiency came, again at University of New South Wales, by combining the earlier developments in the PESC sequence with the front and rear oxide passivation first demonstrated in the rear point contact cell. This is possible in a number of ways as shown in (FIG.3.4). In the PERC (passivated emitter and rear cell) of (FIG.3.4a), the first to be successfully demonstrated, rear contact is made to the silicon substrate through holes in the rear passivating oxide. This approach works reasonably well provided the substrate is sufficiently heavily doped for contact resistance between the metal and substrate. He PERC is often suggested as a relatively low cost way for making silicon cells above 20% efficiency, since it is the simplest of the approaches of (FIG.3.4).

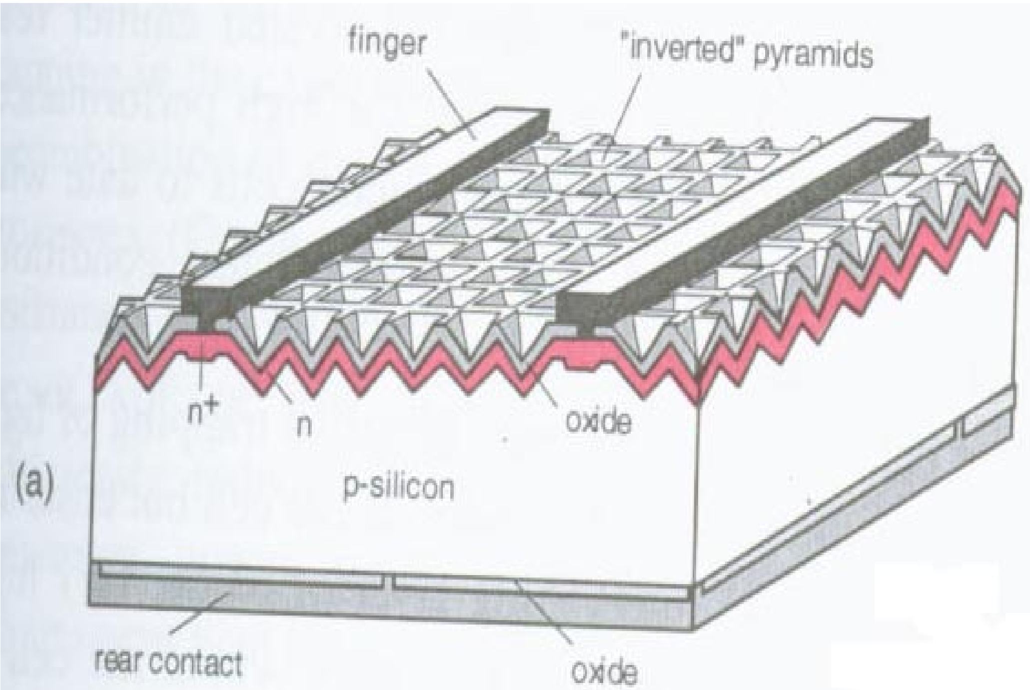

(a)

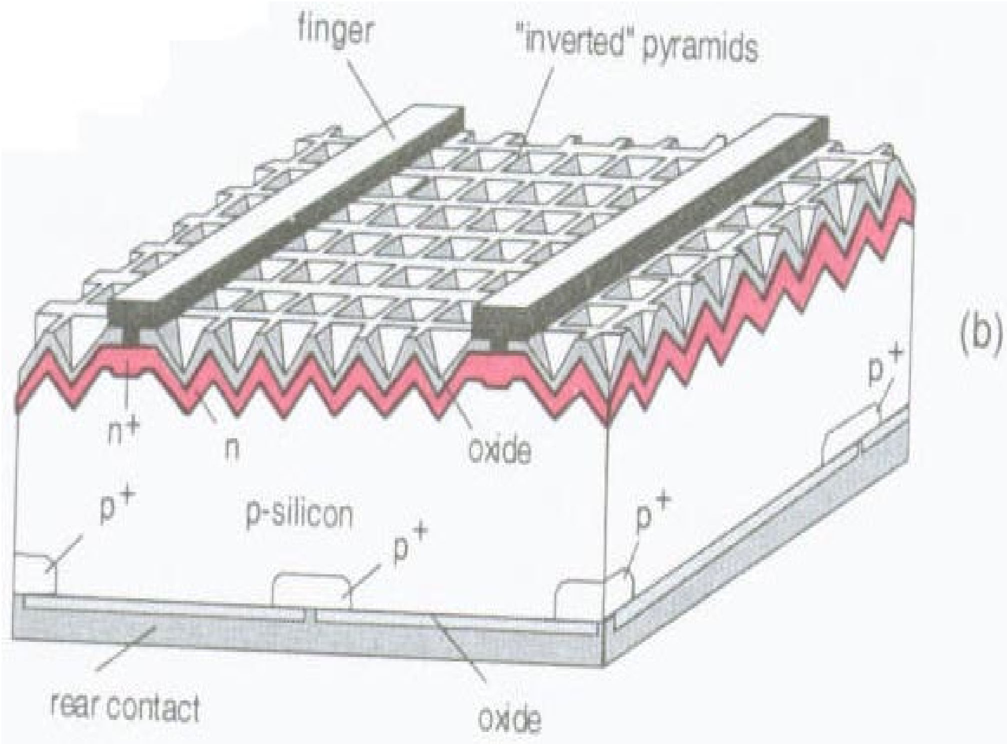

(b)

Figure (3.4) (a) The passivated emitter and rear cell (PERC cell); (b) The passivated emitter, rear locally diffused cell (PERL cell) which took efficiency above 24% in the early 1990s. Source: Green and Hansen (1998).

HOW WILL CELL DESIGN EVOVLE IN THE FUTURE?

It’s provided by (Fig.3.5), which shows the calculated intrinsic energy conversion efficiency bounds on single-junction silicon solar cells. In ‘lambertian’ light trapping schemes, the light direction within the cell is randomised allowing path-length enhancements to be quite. The best laboratory cells have demonstrated close to 85% of the achievable efficiency, according to this (Fig.3.5).

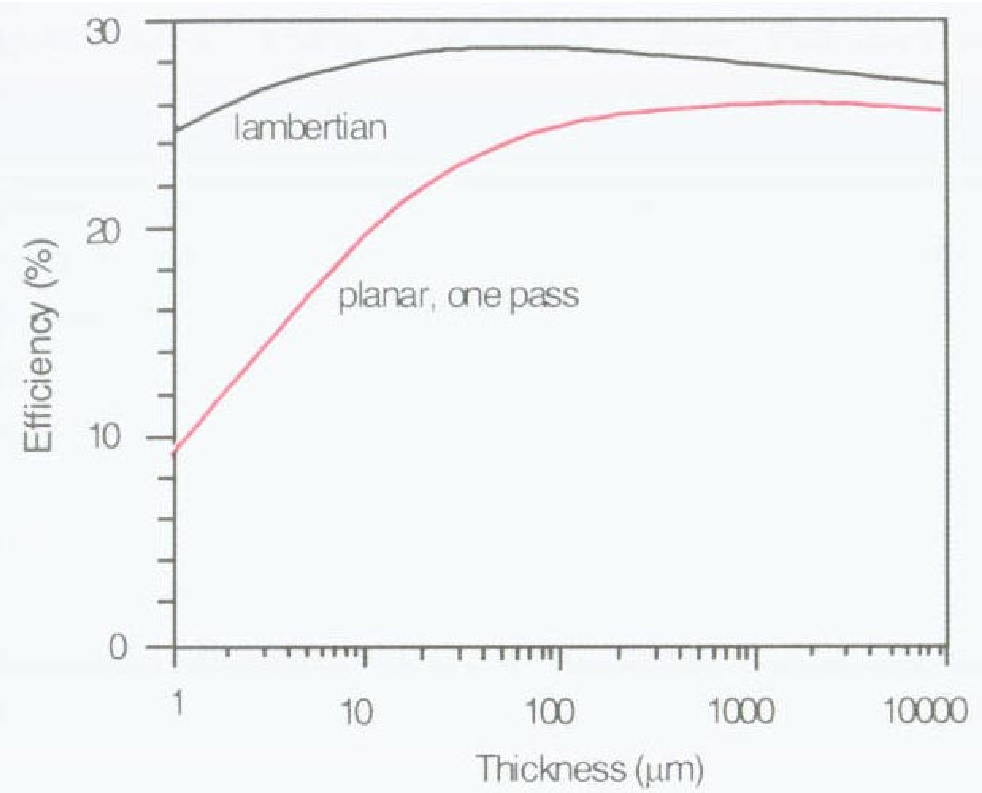

Figure (3.5) Limiting efficiency of a silicon solar cell as a function of cell thickness with and without lambertian light trapping (global AM1.5 spectrum, 100 mW cm^{-2}, 25 C). source: Green (1995).

As opposed to the case of laboratory devices, most manufacturers of commercial cells would be very pleased to be producing consistently cells of half the limiting efficiency of (Fig.3.5). Some of the difference between laboratory and commercial cell performance is due to poorer quality of silicon substrate material.

It seems that eventually it should be feasible to produce low-cost commercial silicon cells of efficiency above 20% with such improved cell designs by paying attention to the passivation of both front and ear surfaces, by thinning the cells to reduce bulk recombination and by modifying the crystal growth processes to withstand high-temperature processing without loss of electronic quality.

An interesting result highlighted by (Fig.3.5), is the way that light trapping allows high performance, in principle, from silicon cells that are 1 μm thick. This provides a justification for expecting very high performance, eventually, from the thin.

3.3-Substrate production

a- Standard process

b- Multicrystalline silicon ingots

c- Sheet and ribbon silicon

3.3.1-standard process

Silicon solar cell technology is capable of benefiting directly from the economies of scale of the silicon microelectronics industry, and also the capable of using scrap material from this industry because he requirements for material quality in photovoltaics are less demanding than in the more general microelectronics field. Accordingly, given the present size relativities, most silicon cells are made from a standard silicon source material originally intended for microelectronics. Over the last ten years, the size relativities have not changed enormously, since both industries have been steadily growing. Explosive growth in the photovoltaics industry, such as that stimulated by urban residential rooftop applications of photovoltaics in 1997, will increasingly upset this delicate balance.

To produce ingots from the pure silicon feedstock, a modification of the Czochralski (CZ) process which produces ‘tricrystalline’ silicon which has been used for photovoltaics (Endros et al., 1997). Another alternative to the standard Czochalski process for producing crystalline ingots is the floatzone (FZ) process. This (FZ) process as commercially implemented has capable of accepting feedstocks only in the form of high quality cylindrical rods. That makes it unsuitable for using low-cost off-grade material. However the casting and directional solidification processes used to produce multicrystalline silicon.

3.3.2- Multicrystalline silicon ingots

In 1998, about 30% of the world’s photovoltaic production was based on multicrystalline silicon wafers. Many companies have developed commercial processes for producing the precursor multicrystalline silicon ingots (Ferrazza, 1996). There are many way to produce the multicrystalline silicon ingots and the advantages over the Czochralski process are lower capital costs, higher throughput and a higher tolerance to poor feedstock quality.

The multicrystalline wafers are capable of producing cells of about 80% of the performance of a monocrystalline cell fabricated on a Czochralski wafer.

3.3.3- Sheet and ribbon silicon

The most advanced sheet or ribbon approach is based on the edge-defined film-fed growth (EFG) technique of (Fig.3.6). As originally developed in the early 1970s this involved the pulling of a thin sheet of silicon ribbon from a strip of molten silicon formed by capillary action at the top of a graphite dye (Fig.3.6). Commercial cells made from edge-defined film-fed growth (EFG) material have been available sporadically since the early 1980s with a large 25MW/yr facility recently announced.

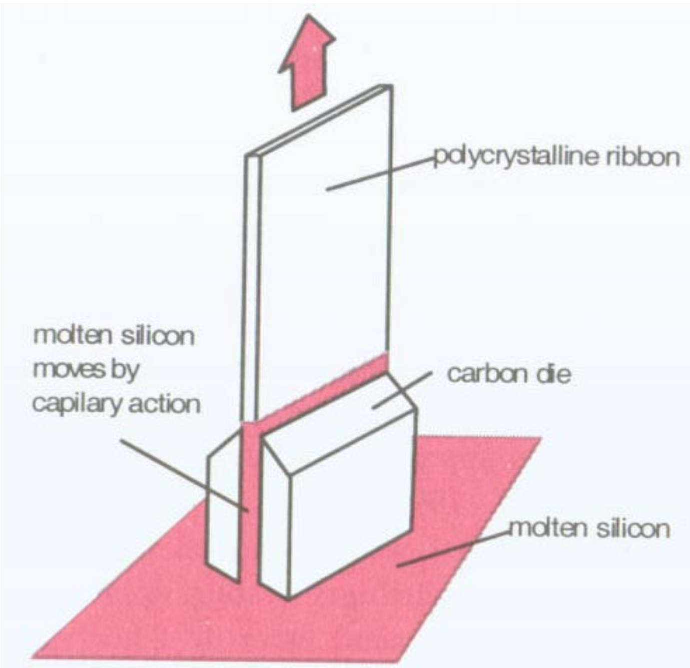

Figure (3.6) Edge-defined, film-fed growth (EFG) method. Source: Green and Hansen (1998).

A somewhat elated approach is the string ribbon approach. In this the molten silicon is trapped between two graphite strings that are drawn from the melt. This relaxes the requirement on thermal control. This approach is under development by Evergreen Solar (Janoch et al., 1997; Wallace et al., 1997).

Another approach, developed in the 1980s, relied on direct casting of silicon wafers using a centrifugal casting approach to overcome surface tension problems within the closely spaced faces of a horizontally aligned graphite mould (Maede and Hide, 1987).

3.4- Cell costs

The cost of the cells is important and there were many studies of silicon cell production using different basic assumptions. Probably the most recent is one conducted under the auspices of the European Union Photovoltaic Program (Bruton et al., 1997).

The key assumptions of the study were manufacturing volume of 500 MW_p of solar cells per annum and the availability of silicon source material at about (US$25 per Kg). A number of different technologies were compared in table 3.1.

Table 3.1 summary of published results of a European Commission study of manufacturing costs for 500 MW_p per year factory

ID	**wafer**[a]	**process**	**Cell efficiency**[b] **study (present)**	**Estimated cost (ECU/W_p)**[c]	**Key variable**
1	DS	SP	15%(12.6-14.8%)	0.91	Wafer
2	CZ	SP	16%(13.9-15.6%)	1.25	Wafer/process
3	CZ	LGBC	18%(16.5-17.5%)	1.15	Process
4	CZ	MIS/A	17%(N/A)	1.28	Process/module
5	CZ	MIS/B	17%(12.2%)	1.34	Module
6	CZ	PERL	20%(N/A)	1.78	Process
7	EFG	SP	14.4%(12%)	0.71	Wafer

Where DS directional solidification; CZ Czochralski growth; EFG edge-defined film-fed growth; SP screen-printed; LGBC laser grooved, buried-contact; MIS/A metal-insulator-semiconductor; MIS/B as for MIS/A but with resin-fill packaging; PERL passivated emitter, rear locally diffused (less appropriate acronym LBSF used in study). b The cell efficiencies assumed in the study in some cases differ appreciably from present average production values, deduced by the present author from manufacturers’ data sheets or the results from large field installations. WHERE (1ECU=US$1.2) Source: Bruton et al., 1997.

From this table it is seen that the screen-printed cells on ribbon (EFG) produces the lowest cost of 0.71 ECU/W_p followed by the multicrystalline wafers at ECU 0.91/W_p. The advantage of the ribbon stems almost entirely from the fact that it doesn’t need to be sawn.

CHAPTER four

PHOTOVOLTAIC MODULES,

SYSTEM AND APPLICATIONS

4.1-photovoltaic modules

In order to provide useful power for application the individual solar cells must be connected together to give the appropriate current and voltage levels and they must also be protected from damage by the environment in which they operate. This electricity connected environmentally protected unit is usually termed a photovoltaic module although it can also be termed a PV laminate when it is supplied without the frame. Figure (4.1) (a) and (b) show typical module constructions for crystalline silicon and thin film silicon cells respectively.

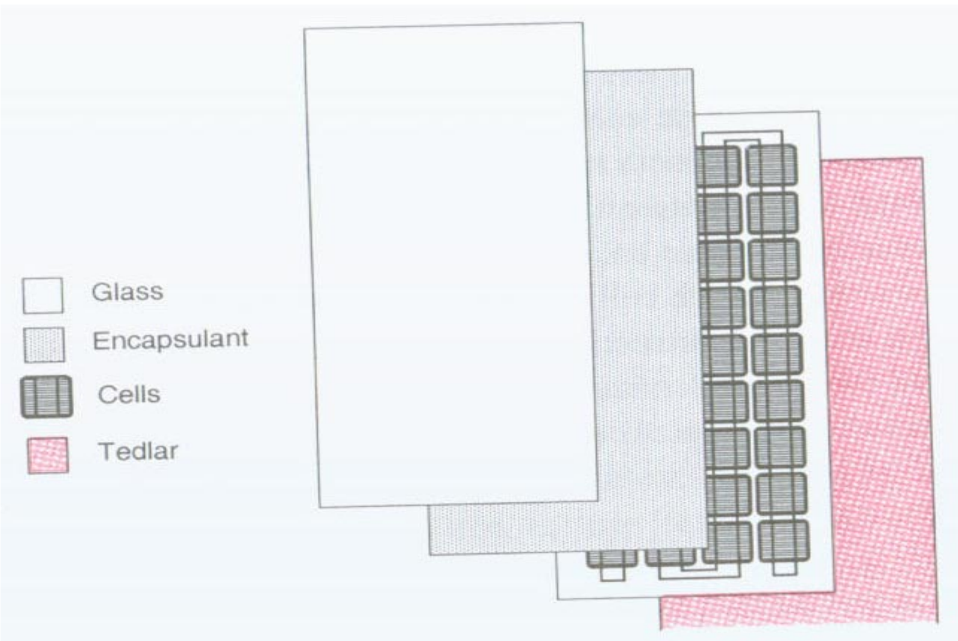

Figure 4.1 (a)

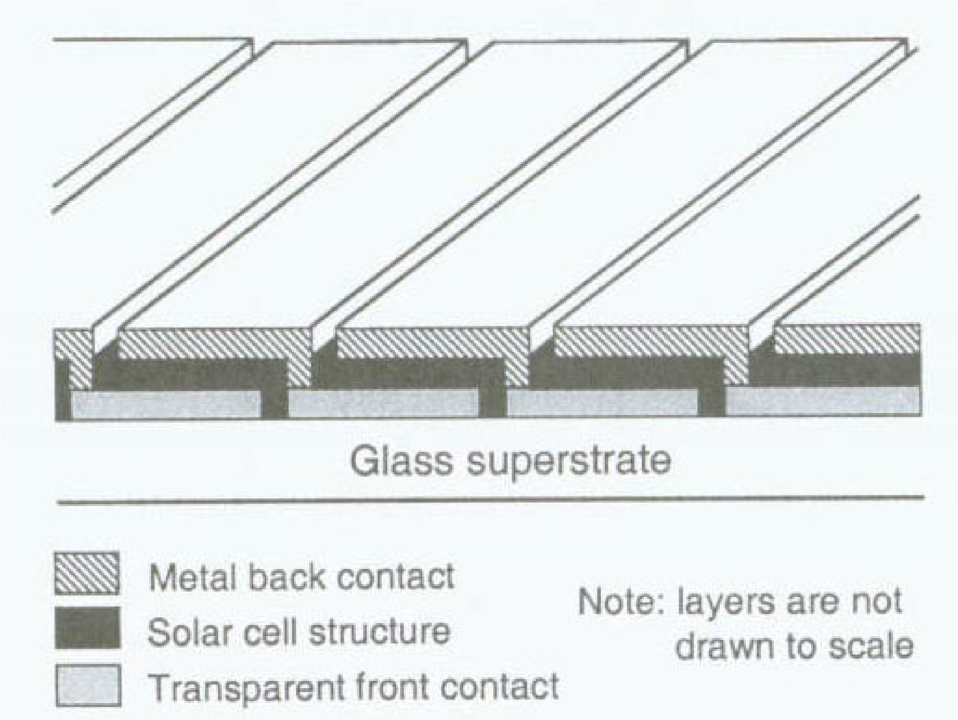

Figure 4.1 (b)

Figure 4.1 a) Schematic of module construction for crystalline silicon cells-exploded view showing the different layers which make up the module; b) Schematic of module construction for thin film cells.

Due to the difference in fabrication process module designs for crystalline and thin film cells, whilst following the same basic principles, differ substantially in several aspects of module construction and design. Indeed, it could be said that the thin film cells are fabricated in modular for requiring only the encapsulation step after completion of the deposition processes. For simplicity the crystalline silicon solar cell will be considered initially in each sub-section since it is presently the most common cell type for power applications. Variations introduced by the use of thin film cells will then be identified.

4.1.1- Electrical connection of the cells

The electrical output of a single cell is dependent on the design of the device and the semiconductor material(s) chosen, but is usually insufficient for most applications. In order to provide the appropriate quantity of electrical power a number of cells must be electrically connected. There are two basic connection methods: series connection in which the top contact of each cell is connected to the back contact of the next cell in the sequence and parallel connection in which all the top contacts are connected together as are all the bottom contacts. In addition connected in a series string to increase the voltage level and in parallel to increase the current level. See figure (4.2)(a, b).

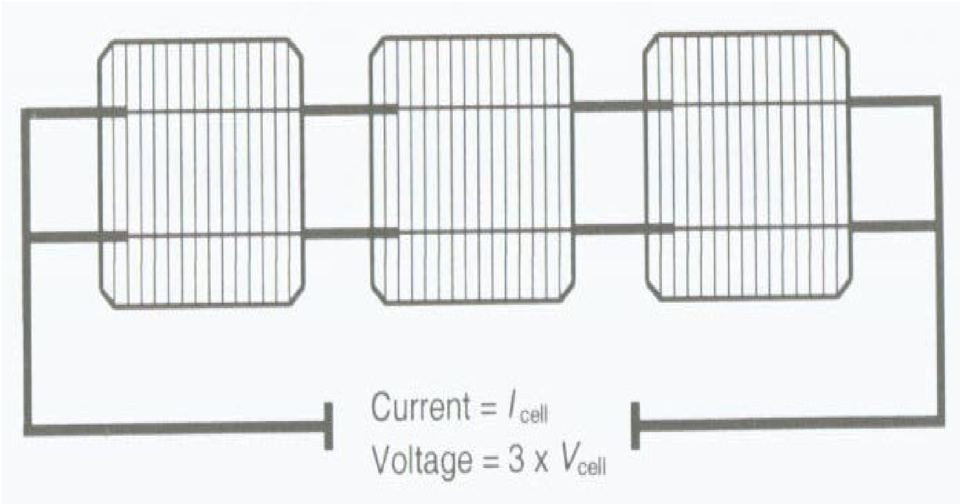

Figure 4.1 (a) Series connections of cells

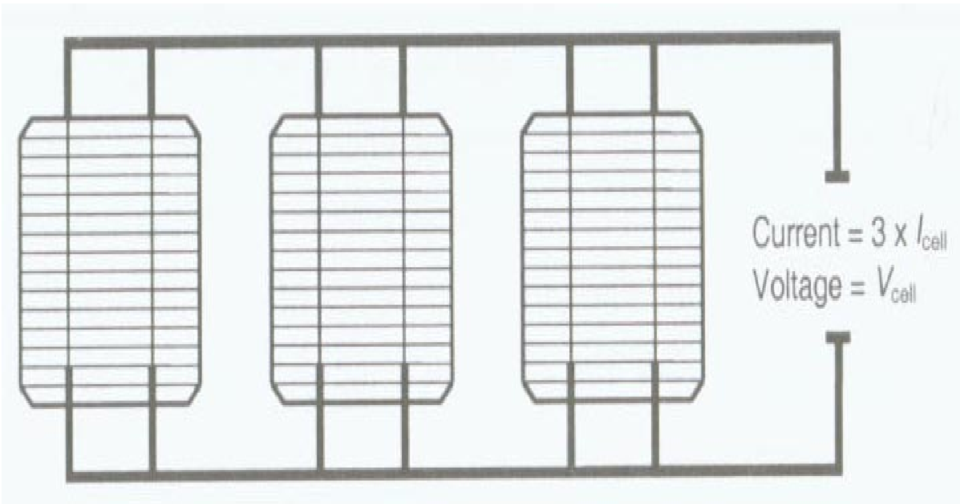

Figure 4.1 (b) parallel connections of cells

4.1.2- Module structure

In modern crystalline silicon modules the front surface is almost always composed of glass, toughened to provide physical strength and with a low iron content to allow transmission of short wavelengths in the solar spectrum. The rear of the module can be made from a number of materials. One of the most common is Tedlar (see Fig.4.3), although other plastic materials can also be used. If a level of transparency is required then it is possible to use either a translucent Tedlar sheet or more commonly a second sheet of glass. The glass-glass structure is popular for architectural applications especially for incorporation into a glazed façade or roof.

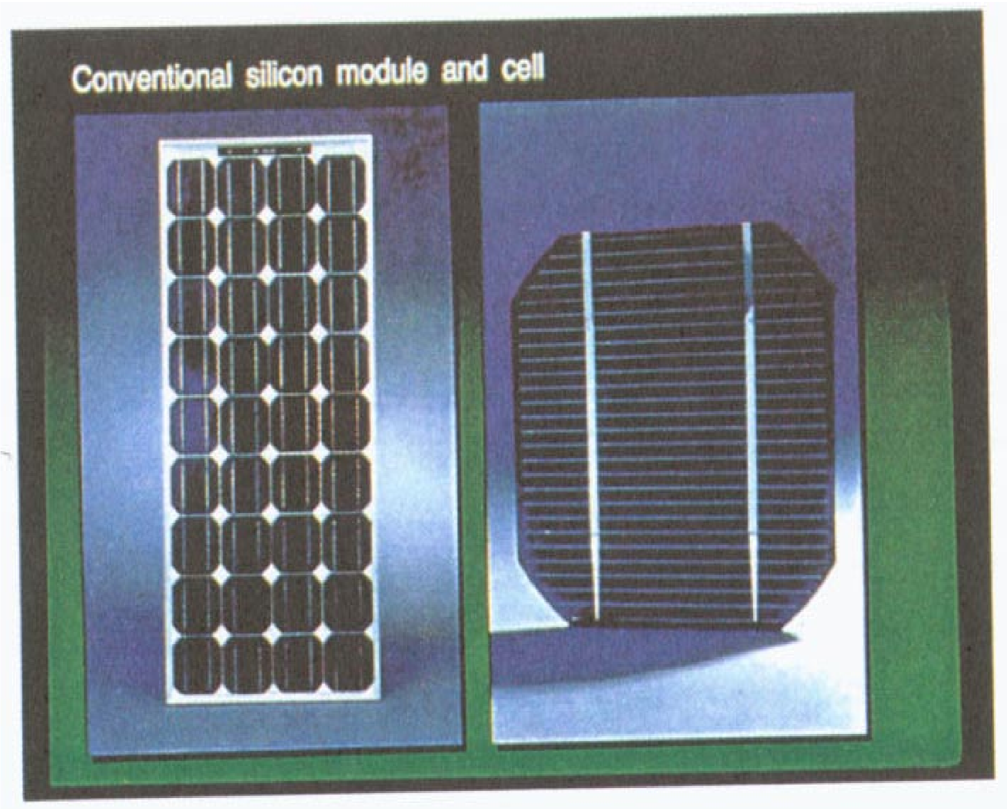

Figure 4.3 Typical crystalline silicon module and cell (photograph courtesy of BP Solarex).

The ideal module would also provide good heat transfer in order to keep the cell temperature as low as possible. However the encapsulant is required to provide electrical isolation and physical protection, so a high heat transfer coefficient is not always possible. The operating temperature is also influenced by the exterior materials of the module, with glass-glass structures usually running at a higher temperature than the glass-Tedlar module under similar conditions.

4.1.3- Variations in module design

Module design varies according to the electrical output required and the application of the PV system. Considerable variation in size, shape, colour and cell spacing has been introduced in recent years to accommodate the consumer market especially where the modules are incorporated directly into the product and the building integration market where appearance is of particular importance. It has also been possible to design modules which have additional functions such as the semi-transparent modules that can be used as shading devices and to influence light patterns inside buildings.

The choice of module structure and design is very dependent on the application in question with output, appearance, cost, compatibility with other components and durability being the issues to consider.

4.2- The photovoltaic array

A PV array consists of a number of PV modules, mounted in the same plane and electrically connected to give the required electrical output for the application. The PV array can be of any size from a few hundred watts to hundreds of kilowatts, although the larger systems are often divided into several electrically independent sub-arrays each feeding into own power conditioning system.

4.2.1- Electrical connection of modules

As with connection of cells to form modules a number of modules can be connected in a series string to increase the voltage level and in parallel to increase the current level or in a combination of two. Matching of interconnected modules in respect of their outputs can maximise the efficiency of the array in the same way as matching cell output maximises the module efficiency.

4.2.2- mounting structure

The main purpose of the mounting structure is to hold the modules in the required position without undue stress.

4.2.3- Tilt angle and orientation

The orientation of the module with respect to the direction of the Sun determines the intensity of the sunlight falling on the module surface. Two main parameters are defined to describe this. The first is the tilt angle which is the angle between the plane of the module and the horizontal. The second one is the azimuth angle which is the angle between the plane of module and due south (or sometimes due north depending on the definition used).

The optimum array orientation will depend on the latitude of the site, the prevailing weather conditions and the loads to be met. The optimum tilt angle is also affected by the proportion of diffuse radiation in the sunlight since diffuse light is only weakly directional. Therefore for locations with a high proportion of diffuse sunlight the effect of tilt angle is reduced.

The final aspect to consider when deciding on array orientation is the incorporation in the support structure. For building-integrated applications the system orientation is also dictated by the nature of the roof in which it is to be incorporated.

4.2.4- Sun-tracking/concentrator systems

Some arrays are designed to track the path of the sun. This can account fully for the sun’s movements by tracking in two axes or can account partially by tracking only in one axis from east to west.

For a flat-plate array, single-axis tracking where the array follows the east-west movement of the Sun has been shown to increase the output by up to 30% for a location with predominantly clears sky conditions. Two-axis tracking where the array follows both the daily east-west and north-south movement of the sun could provide a further increase of about 20% (Lepley, 1990). It is usually more economical to install a larger panel for locations with less than about 3000 hours of direct sunshine per annum.

For concentrator systems the system must track the Sun to maintain the concentrated light falling on the cell. The accuracy of tracking and hence the cost of the tracking system increases as the concentration ratio increases.

4.2.5- Shading

Shading of any part of the array will reduce its output but this reduction will vary in magnitude depending on the electrical configuration of the array.

Thus the reduction in output from shading of an array can be significantly greater than the reduction in illuminated area since it results from

- The loss of output from shaded cells and modules;
- The loss of output illuminated modules in any severely shaded strings that cannot maintain operating voltage;

- The loss of output from the remainder of the array because the strings are not operating at their individual maximum power points.

4.3- The photovoltaic system

The design of the photovoltaic system depends on the task it must perform and the location and other site conditions under which it must operate.

4-3.1- System design

There are two main system configurations- stand-alone and grid-connected. In the stand-alone system operates independently of any other power supply and it usually supplies electricity to a dedicated load or loads. It may include a storage facility (e.g. battery bank) to allow electricity to be provided during the night or at times of poor sunlight levels. By contrast the grid-connected PV system operates in parallel with the conventional electricity distribution system. It can be used to feed electricity into the grid distribution system or to power loads which can also be fed from the grid.

It is also possible to add one or more alternative power supplies (e.g. diesel generator, wind turbine) to the system to meet some of the load requirements. These systems are then known as ‘hybird’ systems. This system can be used in both stand-alone and grid-connected applications but are more common in the former because provided the power supplies have been chosen to be complementary they allow reduction of the storage requirement without increased loss of load. See Figure (4.4) (a, b, c).

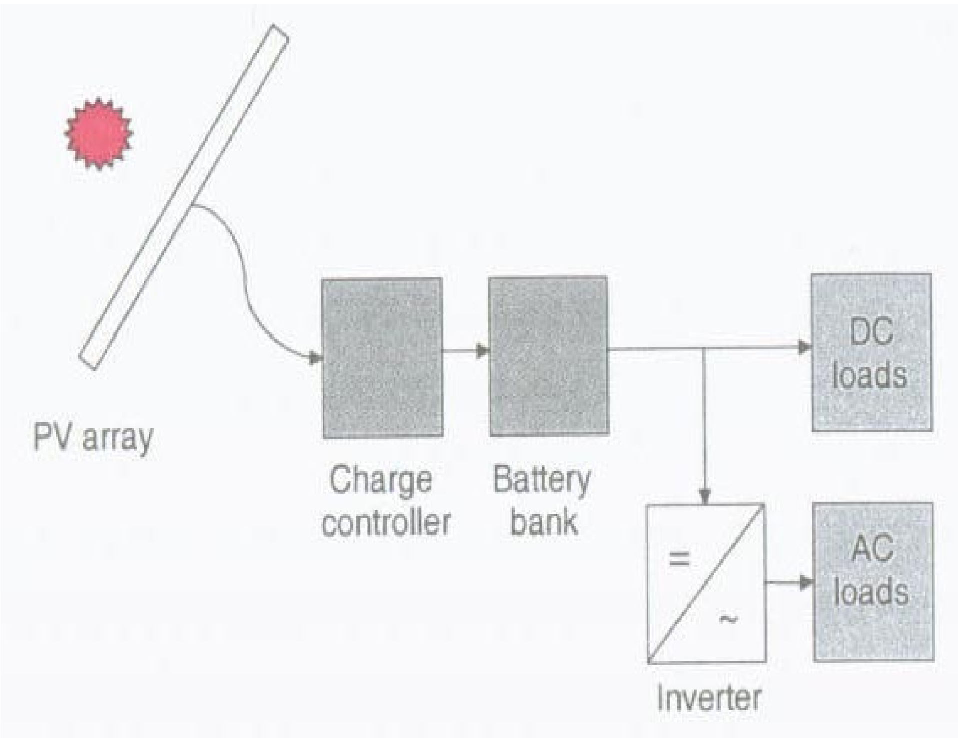

Figure 4.4 a) Schematic diagram of a stand-alone photovoltaic system.

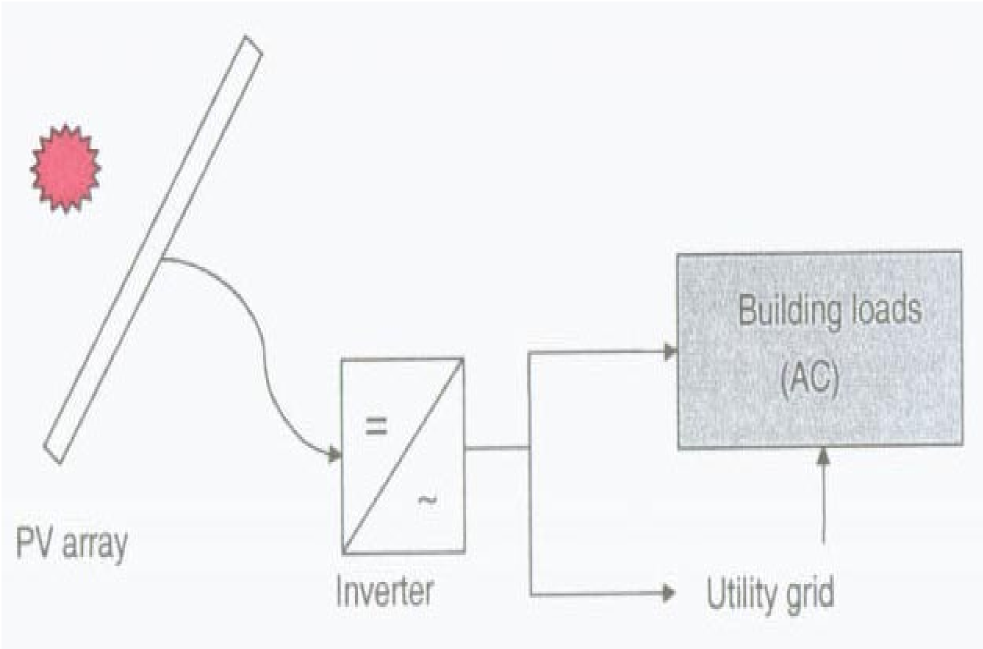

Figure 4.4 b) Schematic diagram of grid-connected photovoltaic system.

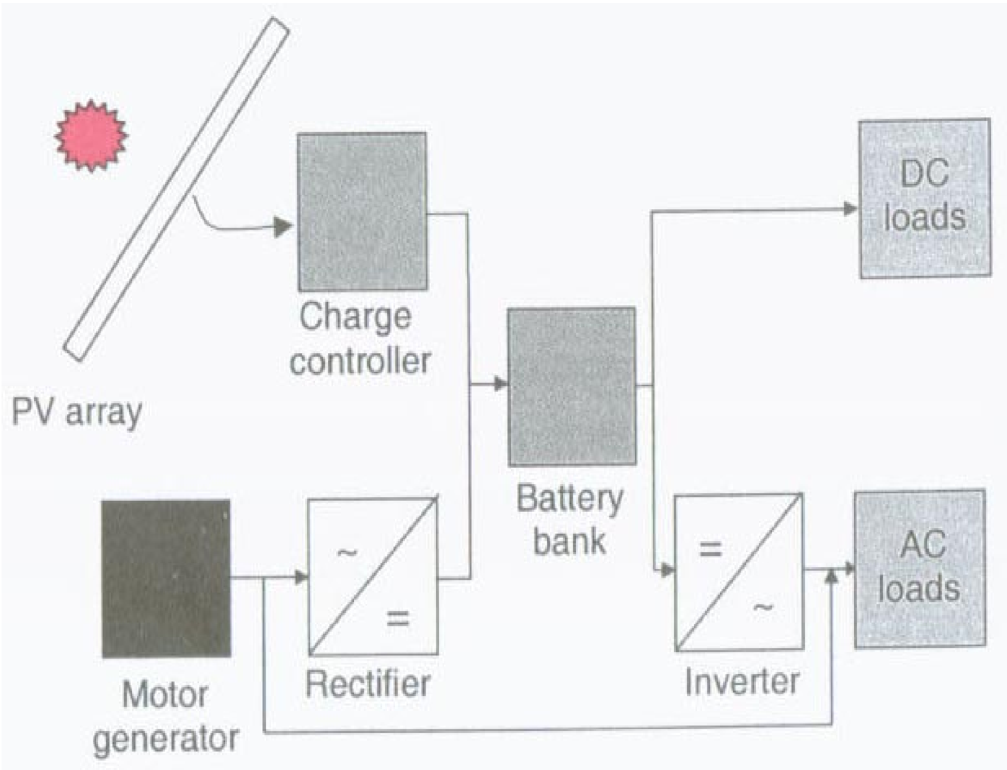

Figure 4.4 c) Schematic diagram of hybrid system incorporating a photovoltaic array and a motor generator (e.g. diesel or wind).

4.3.2- System components

The main system components are the photovoltaic array, power conditioning and control equipment, storage equipment (if required) and load equipment.

The photovoltaic array

The PV array is made up of the PV modules themselves and the support structure required to position and protect the modules.

Power conditioning

It is often advantageous to include some electrical conditioning equipment to ensure that the system operates under optimum conditions. In the case of the array the highest output is obtained for operation at the maximum power point. Since the voltage and current at maximum power point vary with both insolation level and temperature, it is usual to include control equipment to follow the maximum power point of the array, commonly known as the maximum power point Tracker

(MPPT). The MPPT is an electrical circuit which can control the effective load resistance which the PV array sees and thus control the point on the I-V characteristic at which the system operates. There are a number of ways in which the optimum operating point can be found but an MPPT often operates by checking the power levels on either side of the present operating point at regular intervals and if a gain in power is observed in one direction then the MPPT moves the operating point in that direction until it reaches the maximum value. For grid-connected systems the MPPT is often incorporated into the inverter for ease of operation, although it is possible to obtain the MPPT as an independent unit.

Inverter

If the PV system needs to supply AC alternative current loads then an inverter must be included to convert the DC direct current output of the PV array to the AC output required by the load. As with PV systems inverters can be broadly divided into two types these being stand-alone and grid-connected.

The stand-alone inverter is capable of operating independently from a utility grid and uses an internal frequency generator to obtain the correct output frequency (50/60). By contrast the grid-connected inverter must integrate smoothly with the electricity supplied by the grid in terms of both voltage and frequency.

When the inverter is grid-connected it must be ensured that the system will not feed electricity back into the grid when there is a fault on the grid distribution system. The problem is known as islanding and safeguards are required in order to provide protection for equipment and personnel involved in the correction of the fault.

Storage

For many PV system applications, particularly stand-alone, electrical power is also required from the system during hours of darkness or periods of poor weather conditions. In this case storage must be added to the system.

Load equipment

The nature of the load equipment will determine the need for and suitability of the power-conditioning equipment and the capacity of both the PV system and the storage. The first consideration is whether the load or loads use DC or AC electricity. In the former case the loads can be operated directly from the PV system or battery storage whereas AC loads will require an inverter to be included in the system.

Cabling and switching equipment

The array cabling ensures that the electricity generated by the PV array is transferred efficiently to the load and it is important to make sure that it is specified correctly for the voltage and current levels which may be experienced. Since many systems operate at low voltages the cabling on the DC side of the system should be as short as possible to minimise the voltage drop in the wiring. Switches and fuses used in the system should be rated for DC operating. In particular DC sparks can be sustained for long periods leading to possible fire risk if unsuitable components are used.

4.3.3- System sizing

It is important to determine the correct system size in terms of both peak output and overall annual output in order to ensure acceptable operation at minimum cost. If the system is too large it will be more expensive than necessary without increasing performance levels substantially and therefore the system will be less cost-effective than it could be. However if too small a system is installed the availability of the system will be low and he customer will be dissatisfied with the equipment. Again the cost-effectiveness is reduced.

Although many of the same principles are included in the sizing process the approach differs somewhat for stand-alone and grid-connected systems. The first step is to gather the relevant information on he location and purpose of the system.

Location information includes

- Latitude and longitude;
- Weather data-monthly average sunlight levels ambient and maximum temperatures, rainfall, maximum wind speeds, other extreme weather conditions;
- Constraints on system installation-tilt angle, orientation, risk of shading

Information on system purpose includes

- Nature of load or loads;
- Likely load profile-daily, annual variation (if any);
- Required reliability-ability to cope with loss of load (for example clinic lighting required a higher level of demand-many systems fail because they are sized for an existing load, but demand increases soon after provision of the PV supply.

If an autonomous system is required the PV system must provide sufficient electricity to power the loads even under the worst conditions. Thus system sizing is usually carried out for the month that represents the worst conditions in terms of the combination of high load levels and low sunlight conditions.

For a given system design the average electrical output in the sizing month can be calculated from the average daily insolation level (usually expressed in KWh m^{-2}) taking into account he number of modules, their rated efficiency, the efficiencies of all control and the power conditioning equipment, the efficiency of any storage system, mismatch losses, wiring losses and the operating temperature. For an autonomous PV system, the average daily electrical output should match or exceed the average daily load. If his is not the case then the PV array size must be increased.

The battery storage allows for variations in the load level during the day and the provision of power at night. The battery bank must be sized to accommodate the average daily need for electricity which cannot be directly supplied by the PV system and so that this results in only a shallow discharge of the batteries.

Clearly the sizes of the PV array and battery bank are linked and an increase in the size of one can often allow a decrease in the size of the other. The size operating is usually an iteration of the problem to find the most cost-effective solution taking into account the requirements and preferences of the user. Most companies have their own computer programs for performing this iteration and also use their experience to determine the parameters which should be input for any given case. It is also possible to purchase sizing software from several companies.

Therefore most sizing packages are used to determine potential output and to compare different options of system location and design rather than optimising system size as such. Not all sizing packages are suitable for building-integrated applications because they do not take account of the higher operating temperatures or the shading levels which can be experienced. However more complex system simulation programs taking these factors into account have been developed in recent years (see for example, Reise and Kovach, 1995).

4.3.4- System operation

The output of any PV system depends mainly on the sunlight conditions but can also be affected by temperature, shading and the accumulation of dirt on the modules. The overall system performance is usually represented by the efficiency which is defined as the ratio of the electrical output (in KWh) to the sunlight energy input (also in KWh) over the surface of the array in the same period. In general this overall efficiency results from several processes to which individual efficiency values can be assigned, e.g. the conversion of sunlight to DC electricity, the conversion of DC to AC by the inverter.

The system yield is also a useful parameter. This expresses the annual output (or that over another defined period) as a function of the nominal rating of the system and is in units of KWh/KW_p. this allows comparison of systems in different locations. However since this parameter does not explicitly include the sunlight level received over the period, account must be taken of whether the level was above or below average if the yield is to be used for a critical assessment of system performance.

Another often-quoted parameter is the performance ratio which is either given as a percentage or as a number between zero and one. Essentially this parameter expresses the performance of the system in comparison to a lossless system of the same design and rating at the same location. It provides a measure of the losses of the system but because the sunlight level is included in the calculation it becomes independent of sunlight conditions. The performance ratio (PR) is calculated from the following formula:

PR = system output over period / (average daily irradiance x array rating x number of days in period x monitoring fraction)

Where all parameters are values for the same period, the system output is in KWh, the average daily irradiance is in KWh $^{m-2}$ and the array rating is in KW_p. The monitoring fraction is the fraction of the period considered for which monitoring data are available and have been used to determine the values of the other parameters. The formula makes the assumption that average conditions are experienced for the time when data are not collected and so care must be taken with the use of PR values calculated for monitoring fractions less than (0.9).

4.3.5- Operating and maintenance

Because of its lack of moving parts and simple connections, a PV system generally requires little maintenance. However it is necessary to ensure continued access to sunlight by cleaning the panels at appropriate intervals by refraining from building any structures that could shade the panels and by cutting back any branches or other vegetation hat could cover the system. The electrical connections should also be checked at regular intervals to eliminate any problems e.g. corrosion, loose connections. If included in the system the battery bank may need regular maintenance according to the type chosen.

The requirement for cleaning is often overestimated by those with little experience of PV systems. In most cases it can be assumed that 3-5% of performance will be lost if the system is only cleaned annually with up to half of that loss being experienced within a few week of cleaning. However the losses incurred and thus the requirement applications operating under similar condition. For example if there is the possibility of dust or sandstorms causing accumulation on the modules perhaps in a desert area installed in industrial areas close to sources of airborne pollutants. For building integrated systems on houses in many parts of Europe, it may not actually be necessary to clean the systems since the action of rainwater on the inclined panels removes surface dust.

Most operational problems occur as a result of poor maintenance of the BOS components (including loads and batteries) or allowing the array to become obscured or damaged. This latter problem indicates a lack of understanding of the operation of system correctly. This is also demonstrated by system failures arising from the addition of loads that were not included in the original system sizing. In this case the combination of the PV and storage system cannot meet the increased demand and there is a danger of damage to the batteries from deep discharging.

4.3.6- Photovoltaic applications

Two particular examples will be discussed. First, remote area power supplies (RAPS); second building-integrated photovoltaic (BIPV) systems. These represent two of the major markets for photovoltaics, both now and in the future. They also provide examples of stand-alone and grid-connected applications respectively.

Remote area power supplies (RAPS)

These systems supply electrical power to a wide variety of loads remote from any utility distribution grid. The systems range in size from a single module powering a Solar Home System (SHS) to a few kilowatts of PV supplying a local area grid network. The systems are autonomous and so must include energy storage of some sort to supply power in the absence of sunlight. The economics of storage dictate that for larger systems and for those where high reliability is paramount, some of the energy storage will be in the form of fuel for an internal combustion engine. In locations where the seasonal availability of wind energy is complementary to that of the solar irradiance, it is often cost-effective to include a wind turbine in the hybird system.

In a small non critical system such as a small home system (SHS) a PV module charges a battery during the day and the power is used at night for a few high-efficiency lights and a radio or small TV. A charge controller ensures that the battery is not overcharged or deep-discharged, to provide as long a battery lifetime as possible. System sizing is simple using estimates of average daily usage of the loads and in the absence of 10 years of solar data in most locations, estimates of solar irradiance and its variability. In order to keep costs as low as possible a standard system is sold to all users although richer households may purchase a ‘2 module system’, i.e. double the standard system. The reliability of the systems depends to a large extent on the users observing the remaining battery charge from indicator lights on the charge controller and modifying their usage accordingly. A longer than average period of low irradiance will result in a loss of power to the loads but this is an inconvenience to the users rather than a threat to life or to the system.

Some autonomous systems are part of safety-critical networks for instance in aircraft navigation aids or telecommunication systems. In these cases it is permitted to lose power to the loads only one day in 100 years and the system design must guarantee this very low loss-of-load probability (LOLP). Even if there were long-run, accurate solar data for the site, it must be remembered that the stochastic variability of solar irradiance is such that past data are only an average predictor for the future and once in 10 year events are not predictable (Lorenzo and Narvarte, 2000). It is always possible to oversize the PV array and battery to give such a LOLP in an average 10 year period, at a high cost but even then there is no guarantee that a 1-in-100 year low or worse will not occur in the first year of operation. The cost-effective solution is to include additional charging from a small internal combustion engine, usually a diesel, with a fuel store large enough to need refilling only on visits to the site for periodic maintenance of the electronic systems. The PV array and battery system are sized so that the engine is run at full power for about 1 hour/day, to keep it in good condition.

The PV/diesel hybird system is used in many parts of the world as an alternative to grid extension. In Australia farms and small communities in the outback are supplied with a RAPS system in a standard container unit. All parts are transported in the container which on location becomes the base for the system. The PV array is mounted on the roof with the diesel engine, batteries and all power conditioning and controls mounted inside the container. The daytime load is supplied by the PV system, with the diesel engine as a back-up charger for the supply of night-time loads. The diesel engine is run at full power for at least one hour per day, to maintain it in good condition without excessive use of fuel. The fuel tank is sized so to need refilling only at long intervals so reducing the transport cost of the fuel.

Remote area power supplies make use of the fact that sunlight is freely distributed to all sites however remote (at least in the Sunbelt). The challenge in system design is to match the power output to the load as far as possible and maintain a very high availability for safety-critical systems whist keeping costs as low as possible. Storage is essential for any system that has a night-time load and while battery storage remains expensive it will be cheaper for system over $500W_p$ or so to include a diesel engine.

Building-integrated photovoltaic (BIPV) system

One of the fastest growing sectors of the photovoltaic market is the building integrated photovoltaic system.

This is an ideal application for the use of photovoltaics in an urban environment and takes advantage of the distributed nature of sunlight and of the electrical load. The benefits of the BIPV system can be summarised as follows:

- in common with other PV systems and most renewable energy technologies, it has a lower environmental impact than production of electricity from conventional fuels;
- the electricity is generated at the point of use so reducing the impact and cost of distribution;
- there is a possibility of offsetting some of the cost of the PV array by the amount which would have been paid for the building material it has replaced;
- the system does not require additional land area since building surfaces are used to accommodate the array.

The PV modules can be integrated in several different ways for example to replace roofing tiles, in place of façade material or as sunshades. (Figure 4.5) shows an example of façade integration but there are many different ways of including the PV array in the building design.

Figure 4.5 Example of façade integration of photovoltaics. The photograph shows the 40 kW_p PV façade on Northumberland Building at the University of Northumbria. The PV array is integrated into the rainscreen overcladding. This system was installed in 1994 and is one of the early examples of façade integration (photograph courtesy of University of Northumbria).

The principle of the technical system design is similar to that for other PV applications but there are some additional aspects to be taken into account. It may be designed to match the general load profile or to provide higher output levels when, for instance, air conditioning is required but it does not need to be an autonomous system since most of the buildings also have a grid supply.

However the area available for the BIPV array may be constrained by building design, shading from surrounding structures or owner preference. Thus the system size is often dictated by the nature of the building rather than its electrical loads. The visual aspect of the system is also important and this often affects the choice of module type, location and detailed integration method. Finally he system design must take into account ease of installation, maintenance and operation and compliance with building regulations.

The heat at the rear of the modules can also be used in some cases. Even in the most efficient modules, only about 15% of the light falling on the module is turned into electricity and whilst a few percent is reflected, the rest is absorbed as heat. This results in a module operating temperature that can be 25-50 k above ambient temperature. Reducing the operating temperature by removing some of the heat is advantageous in terms of increasing system efficiency and a double benefit can be obtained if the heat is useful for another purpose.

Because of the rather large area of the module and the relatively modest temperature differential between the module and ambient temperatures, it is not usually cost effective to use forced air or fluid flow to extract the heat unless three is a direct use for that heated air or fluid. However, the heat can be used to assist natural ventilation within the building by taking in cold air at the bottom of the building. As this air is heated behind the PV façade, it rises and pulls in more cold air to replace it. Examples of such ventilation systems include the Doxford Solar Office in the UK (Lloyd Jones et al., 1998) and the Mataro library in Spain (Lloret et al., 1997).

Even for a system where no use is made of the heat, care must be taken to ensure that the PV array operating temperature remains at an acceptable level. For most stand-alone systems there is free air movement around the array and so some cooling is effected. This is not the case for a BIPV system which forms pat of the building fabric. The design must include adequate ventilation around the modules if significant losses in efficiency are to be avoided.

Most BIPV systems are grid-connected with the conventional electricity supply meeting any shortfall between the BIPV electrical output and the building demand. The system must conform to safety regulations for connection. There is a wide range of tariffs offered for this electricity, ranging from the replacement generation cost to several times the normal electricity rate where a scheme to promote BIPV exists (more information in Haas, 1998).

Several countries (e.g. Germany, the Netherlands and USA) have major promotion schemes for BIPV stimulated by environmental concerns over global warming and pollution.

4.4-Costs of PV components and system

The generation of electricity from PV systems is unlike that of other systems in that the cost of generation is only weakly dependent on the size of the system. This is a result of the modularity of PV systems and such differences as do exist at present arise mainly from sales installation and maintenance costs rather than hardware costs. These costs will fall as the throughput of PV systems in the supply, installation and maintenance chains increases with increased sales.

The cost of manufacturing a PV module consists of the material, labour, capital and energy costs. The purchase price of a module is of course higher since it must also include marketing and sales costs, the profits to manufacturer and supplier and the costs of management and other overheads. The price of materials falls as they are purchased in tonnes rather than kilograms, whilst large-scale production uses machinery rather than labour so that the labour costs/unit also falls. The capital cost of equipment to make 1 million modules per year is much less than 10 times the cost of equipment to make 100000 per year, the equipment would occupy much less than 10 times the space and it would use much less than 10 times the energy. It is also the case that large companies can borrow money more cheaply than small ones so the capital repayments/unit of borrowing become smaller as the PV industry grows, further reducing the capital costs of manufacture.

The cost of a PV system is the sum of the costs of the hardware and the costs of transport, system design, installation and maintenance. The price paid by a customer also includes the mark-up of the wholesaler and retailer in many instances and often must included taxes and duties.

The non-hardware costs also have benefits of scale. The unit cost of transport is lower for a container load than for a small number of modules or systems. Spreading design costs over large numbers of systems reduces the cost to each system, whilst the installation and maintenance of many systems/year in one locality reduces the cost per system. The increasing market for PV system will therefore lead to a reduction in all of the system costs.

One of the most interesting applications for PV is on buildings where building integrated PV (BIPV) systems can effectively result in no additional cost. When PV modules are integrated into the structure of a building they have a dual function. They act as a building element, replacing a conventional roof or façade as well as being a generator of electricity. On houses the BIPV system replaces roof tiles which are of relatively low cost. On commercial office buildings, however, the BIPV system replaces the cladding elements that ensure both the weather-tightness of the building and its physical appearance. Conventional cladding systems vary widely in cost but for luxury cladding such as polished stone, the cost can be over £1000/m^2. Where a BIPV system replaces such cladding, the cost of the building is lower with PV than with the polished stone and the owner of the building gets electricity generation at no additional costs.

Property developers use expensive cladding for prestige and companies buy or occupy such buildings to enhance their public image. With the increase in ‘green’ awareness, a BIPV façade on a building can make a very significant public statement for the owners and occupiers of the building and the image value can justify its classification as a luxury cladding. As the cost of PV modules falls then BIPV systems can replace cheaper conventional cladding at zero additional cost and the market for BIPV will expand greatly. The cost of electricity generated by a BIPV system is greatly influenced by the avoided cost of the conventional cladding that is replaced by the PV. Table 4.1 shows the cost of electricity from PV costing £2/W_p about US$3/$W_p$ for a range of cladding under the assumptions specified.

It is clear from Table 4.1 that PV laminates costing £2/W_p and replacing conventional cladding costing £300/m^2 or more can generate electricity at a cost below the retail price from a utility. The electricity is a free by-product if the PV replaces cladding costing £350/m^2 or more. A modest insolation level reasonable for UK facades was chosen to demonstrate that the economic use of BIPV is not only possible for regions with high sunlight levels. Competitive electricity costs would be reached at higher module and/or Balance of System (BOS) costs for locations with higher sunlight levels.

Laminate cost £/m^2	Cladding cost £/m^2	Net PV cost Laminate-Cladding £/m^2	£/W_p	System cost Net PV+BOS £/W_p	Electricity cost pence/KWh
280	100	180	1.3	1.8	27
280	150	130	0.9	1.4	22
280	200	80	0.6	1.1	18
280	250	30	0.2	0.7	10
280	300	-20	-0.14	0.36	5
280	350	-70	-0.5	0	0

Table 4.1 the cost of electricity generated by a BIPV system for a range of cladding costs. Assumption PV laminates: efficiency 14% cost£2/W_p; BOS costs £0.5/W_p; insolation 700 KWh $m^{-2}yr^{-1}$; discount rate 8%; lifetime 30 years.

CHAPTER 5

(EXPERIMENT IN LABORATORY OF STRATHCLYDE UNIVERSITY)

(EXPERIMENT IN LAPORATORY OF STRATHCLYD UNIVERCITY)

This chapter presents and discusses the experiments performed inside the laboratory. The system consisted of:

- solar *simulator* calibration
- Monocrystalline photovoltaic module
- instruments to measure the temperature
- instrument to measure the current and voltage

-solar simulator calibration

In order to calibrate the PV module, the calibration of the solar simulator was required. The Strathclyde University solar simulator consists of 50 tungsten halogen's lamps, type PRA 38, manufactured by Thorn Lighting LTD; see figure 5.1. Irradiance varies from point to point. The framework for the lamps is held by threaded ropes and pulleys which are fixed to the ceiling of the simulator room. The distance between the lamps and the test area can be varied by lowering or raising the frame.

The distance between the solar simulator calibration and the PV module is more or equal one metre in order to obtain uniformity of illumination.

Figure 5.1 University solar simulator consists of 50 tungsten halogen’s lamps, type PRA 38, manufactured by Thorn Lighting LTD

Monocrystalline photovoltaic module

The PV module was disconnected from the battery and placed under the solar simulator. The irradiance was varied by varying the electrical voltage to the solar simulator lamps and output (voltage and current) of the module. See figure (5.2)

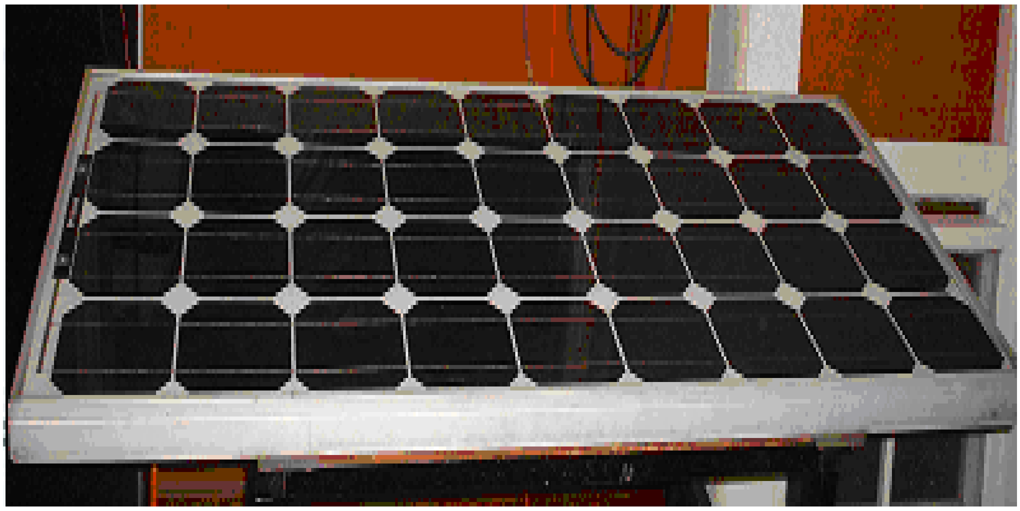

Figure (5.2) monocrystalline photovoltaic module in lap. Of Strathclyde University module type: BP 585 F

Normal peak power (P_{max}) —-- 85.00 watt

Peak power voltage (V_{mp}) --- 18.00 V0lt

Peak power current (I_{mp}) --- 4.72 Ampere

Short circuit current (I_{sc}) --- 5.00 Ampere

Open circuit voltage (V_{oc}) --- 22.03 volt

Minimum power (P_{min}) --- 80.00 watt

Power specifications measured at standard test conditions, insolation of 1000w/m^2, am 1.5, 25 °c cell temperature.

Module certified to CEC Specification 503.

From this information it found the fill factor (F) was found as:

F= V_{mp} * Imp / Isc * Voc

F = 0.7713

Power P = I_{sc} * V_{oc} * F

Instruments to measure open circuit voltage and short cicuit current

There after, the open circuit voltage and short circuit current could be measured. See figure (5.3).

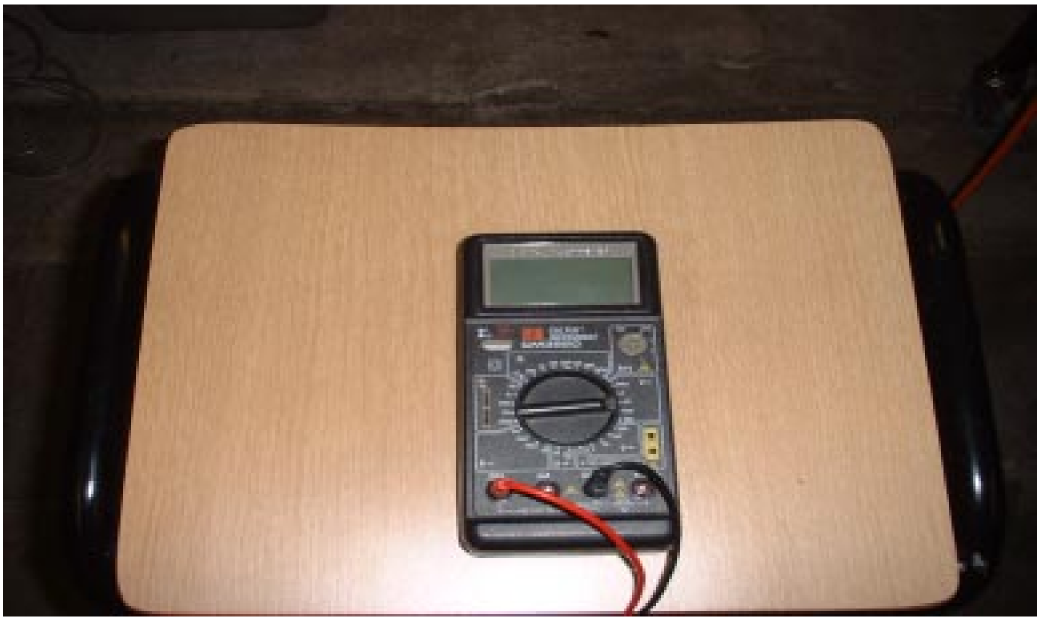

Figure (5.3) Digital Multimeter

Instruments to measure temperature and output voltage current

The temperature at the rear surface of the cell was measured by placing a type K thermocouple (copper constantan) with an attached electrical thermometer. See figure (5.4).

Figure (5.4) Thermometer. The range (-50 °C to 1300 °C) and the accuracy :(±1 °C) for the range (-50°C to 1000°C).

Experimental work

An important performance characteristic of PV systems is the relationship between power output and the cell temperature. The objective of the experiments was to quantify this relationship by plotting power output against the temperature of the photovoltaic module. This was done by irradiating the test panel and measuring its temperature over a series of time steps as the temperature of the cell increased towards the equilibrium value.

The work was carried out in the solar simulator located within the Mechanical Engineering Laboratories at Strathclyde University. The solar simulator and panel used are as described previously.

Two levels of irradiation were used, 500 W/m^2, 600 W/m^2, and 700 W/m^2 and reading were taken at 1 minute intervals.

Experiment (1), irradiance 500 W/m^2:

The solar simulator was run for 50 minutes and readings were recorded at 1 minute intervals

Temperatures recorded

- Air temperature = 20 °c
- Module temperature
- Different in temperature (ΔT) =module temp-air temperature

Electrical power recorded

- V_{oc} (open circuit voltage)
- I_{sc} (short circuit current)

Experiment (2), irradiance 600 W/m^2:

The solar simulator was run for 50 minutes and readings were recorded at 1 minute intervals

Temperatures recorded

- Air temperature = 20 °c
- Module temperature
- Different in temperature (ΔT) =module temp-air temperature

Electrical power recorded

- V_{oc} (open circuit voltage)
- I_{sc} (short circuit current)

Experiment (3), irradiance 700 W/m^2:

The solar simulator was run for 50 minutes and readings were recorded at 1 minute intervals

Temperatures recorded

- Air temperature = 20 °c
- Module temperature
- Different in temperature (ΔT) =module temp-air temperature

Electrical power recorded

- V_{oc} (open circuit voltage)
- I_{sc} (short circuit current)

Results

The results are given in tabular form in Tables 1, 2 and 3.

The results are given in graphical form in figures 5.5, 5.6 and 5.7.

voltage(volt)	current (A)	Temp (Ts)	∆T	power (W)
20	0.57	22	2	8.7894
19.82	0.58	24	4	8.8631076
19.74	0.58	26	6	8.8273332
19.6	0.59	28	8	8.915844
19.49	0.59	30	10	8.8658061
19.4	0.59	32	12	8.824866
19.19	0.6	34	14	8.877294
19.07	0.6	36	16	8.821782
18.91	0.6	38	18	8.747766
18.77	0.6	40	20	8.683002
18.64	0.6	41	21	8.622864
18.57	0.6	43	23	8.590482
18.46	0.6	44	24	8.539596
18.38	0.61	45	25	8.6442978
18.3	0.61	46	26	8.606673
18.24	0.61	47	27	8.5784544
18.19	0.61	47	27	8.5549389
18.14	0.61	48	28	8.5314234
18.08	0.61	49	29	8.5032048
18.04	0.61	50	30	8.4843924
18.01	0.61	50	30	8.4702831
17.98	0.61	50	30	8.4561738
17.95	0.61	51	31	8.4420645
17.91	0.61	51	31	8.4232521
17.87	0.61	52	32	8.4044397
17.84	0.61	52	32	8.3903304
17.8	0.61	52	32	8.371518
17.77	0.61	53	33	8.3574087
17.75	0.61	53	33	8.3480025
17.72	0.61	53	33	8.3338932
17.7	0.61	53	33	8.324487
17.67	0.61	54	34	8.3103777
17.65	0.61	54	34	8.3009715
17.64	0.61	54	34	8.2962684
17.62	0.61	55	35	8.2868622
17.61	0.62	55	35	8.4179322
17.6	0.62	55	35	8.413152
17.58	0.62	55	35	8.4035916
17.57	0.62	55	35	8.3988114
17.55	0.62	56	36	8.389251
17.54	0.62	56	36	8.3844708
17.53	0.62	56	36	8.3796906
17.52	0.62	56	36	8.3749104
17.51	0.62	56	36	8.3701302
17.5	0.62	56	36	8.36535
17.49	0.62	56	36	8.3605698
17.49	0.62	56	36	8.3605698
17.48	0.62	56	36	8.3557896
17.48	0.62	57	37	8.3557896

Table (1) for the input irradiation 500 w and air temp. 20 °c

voltage (volt)	current (A)	Temp (Ts)	∆T	power (w)
20.3	1	22	2	15.6513
20	1.01	24	4	15.5742
19.9	1.01	26	6	15.49633
19.75	1.01	28	8	15.37952
19.58	1.01	30	10	15.24714
19.33	1.02	32	12	15.2015
19.24	1.02	34	14	15.13072
19.04	1.03	36	16	15.12024
18.92	1.03	38	18	15.02494
18.75	1.03	40	20	14.88994
18.64	1.03	42	22	14.80258
18.52	1.04	43	23	14.85008
18.43	1.04	44	24	14.77791
18.34	1.04	46	26	14.70575
18.27	1.04	47	27	14.64962
18.18	1.04	48	28	14.57745
18.13	1.04	48	28	14.53736
18.08	1.05	49	29	14.63666
18.02	1.05	50	30	14.58809
17.96	1.05	50	30	14.53952
17.93	1.05	51	31	14.51523
17.89	1.05	51	31	14.48285
17.84	1.05	52	32	14.44237
17.8	1.05	53	33	14.40999
17.77	1.05	53	33	14.3857
17.75	1.05	54	34	14.36951
17.73	1.05	54	34	14.35332
17.71	1.06	54	34	14.47367
17.68	1.06	54	34	14.44916
17.66	1.06	55	35	14.43281
17.64	1.06	55	35	14.41647
17.61	1.06	55	35	14.39195
17.59	1.06	55	35	14.3756
17.59	1.06	55	35	14.3756
17.57	1.06	56	36	14.35926
17.56	1.06	56	36	14.35109
17.54	1.06	56	36	14.33474
17.53	1.06	56	36	14.32657
17.51	1.06	57	37	14.31022
17.5	1.06	57	37	14.30205
17.48	1.06	57	37	14.2857
17.47	1.06	58	38	14.27753
17.46	1.06	58	38	14.26936
17.45	1.07	58	38	14.39573
17.44	1.07	58	38	14.38748
17.43	1.07	58	38	14.37923
17.42	1.07	58	38	14.37098
17.41	1.07	58	38	14.36273
17.41	1.07	59	39	14.36273

Table (2) for the input irradiation 600 w and air temp. 20 °c

Voc(volt)	current (A)	Temp(Ts)	ΔT	power(w)
20.5	1.31	23	3	20.70521
20.3	1.31	26	6	20.5032
20.1	1.31	30	10	20.3012
19.82	1.32	33	13	20.17121
19.56	1.32	36	16	19.9066
19.26	1.33	39	19	19.74978
19.05	1.33	42	22	19.53444
18.81	1.34	45	25	19.43336
18.63	1.35	47	27	19.39104
18.42	1.35	49	29	19.17246
18.29	1.35	51	31	19.03715
18.12	1.36	52	32	18.99991
18.03	1.36	54	34	18.90554
17.91	1.36	56	36	18.77971
17.82	1.37	57	37	18.82273
17.73	1.37	58	38	18.72767
17.66	1.38	59	39	18.78989
17.58	1.38	60	40	18.70477
17.51	1.38	61	41	18.63029
17.46	1.39	62	42	18.71171
17.42	1.39	63	43	18.66884
17.39	1.39	63	43	18.63669
17.35	1.39	63	43	18.59382
17.33	1.4	64	44	18.706
17.31	1.4	64	44	18.68441
17.28	1.4	65	45	18.65203
17.24	1.4	65	45	18.60886
17.2	1.4	66	46	18.56568
17.18	1.41	66	46	18.67655
17.15	1.41	66	46	18.64394
17.13	1.41	67	47	18.62219
17.11	1.41	67	47	18.60045
17.08	1.41	67	47	18.56784
17.07	1.41	68	48	18.55697
17.04	1.41	68	48	18.52435
17.03	1.41	68	48	18.51348
17.02	1.41	68	48	18.50261
17.01	1.41	68	48	18.49174
16.99	1.41	68	48	18.47
16.97	1.41	69	49	18.44826
16.95	1.41	69	49	18.42651
16.94	1.41	69	49	18.41564
16.93	1.41	69	49	18.40477
16.91	1.41	69	49	18.38303
16.9	1.41	70	50	18.37216
16.89	1.42	70	50	18.49151
16.88	1.42	70	50	18.48056
16.87	1.42	70	50	18.46961
16.86	1.42	70	50	18.45867
16.85	1.42	70	50	18.44772

Table (3) for the input irradiation 700 w and air temp. 20 °c

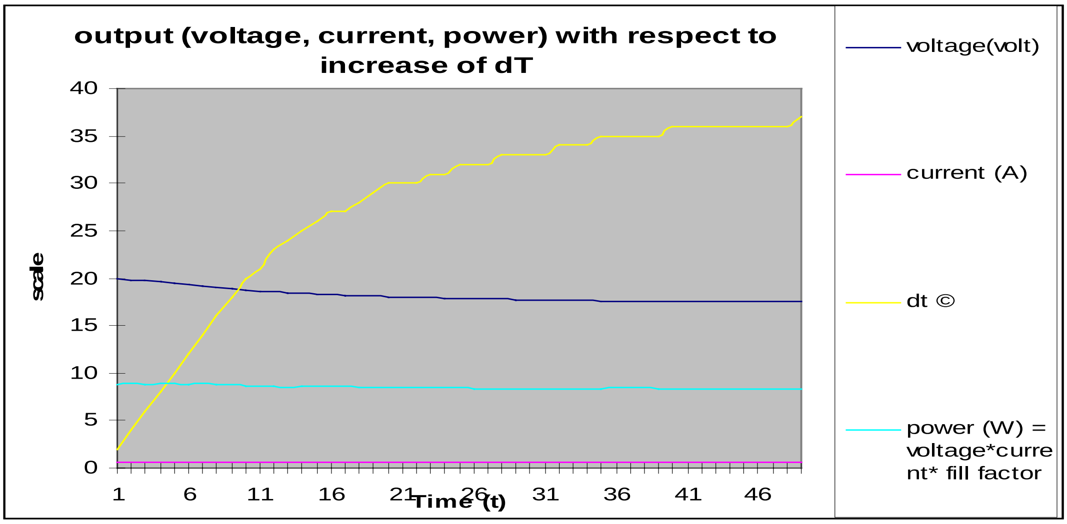
output (voltage, current, power) with respect to increase of dT
scale
Time (t)
voltage(volt)
current (A)
dt ©
power (W) = voltage*current* fill factor

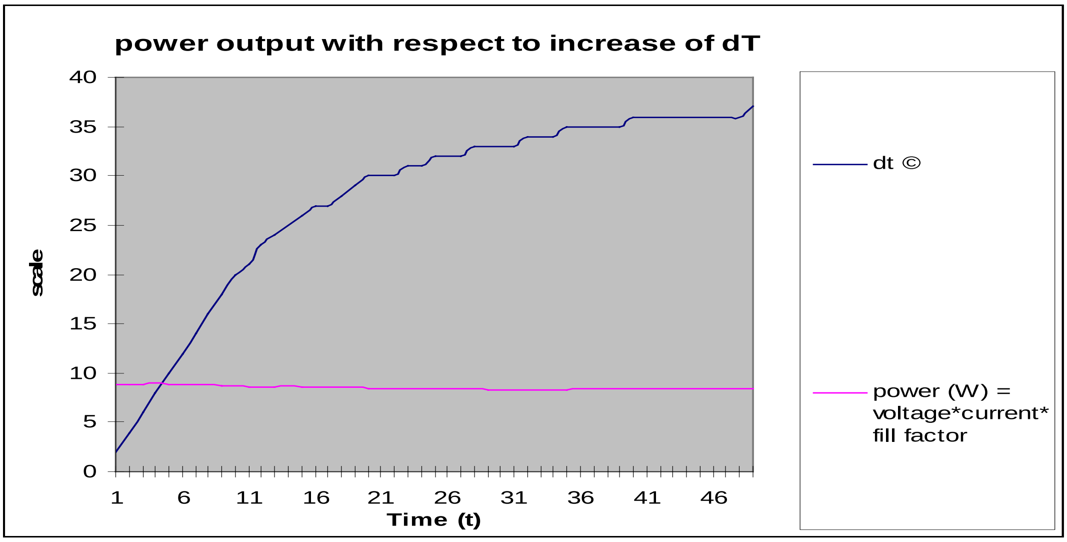
power output with respect to increase of dT
scale
Time (t)
dt ©
power (W) = voltage*current* fill factor

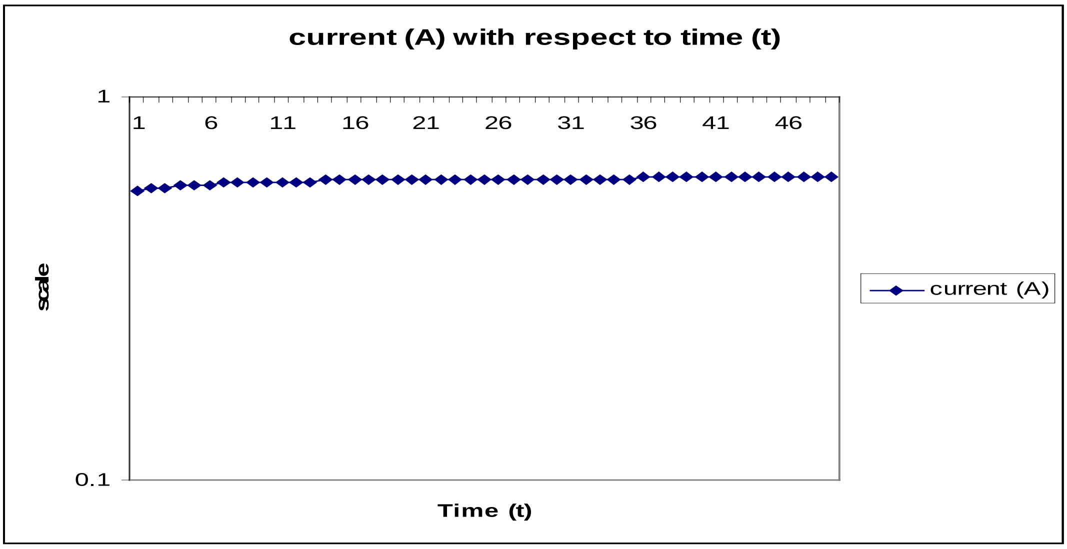
current (A) with respect to time (t)
scale
Time (t)
current (A)

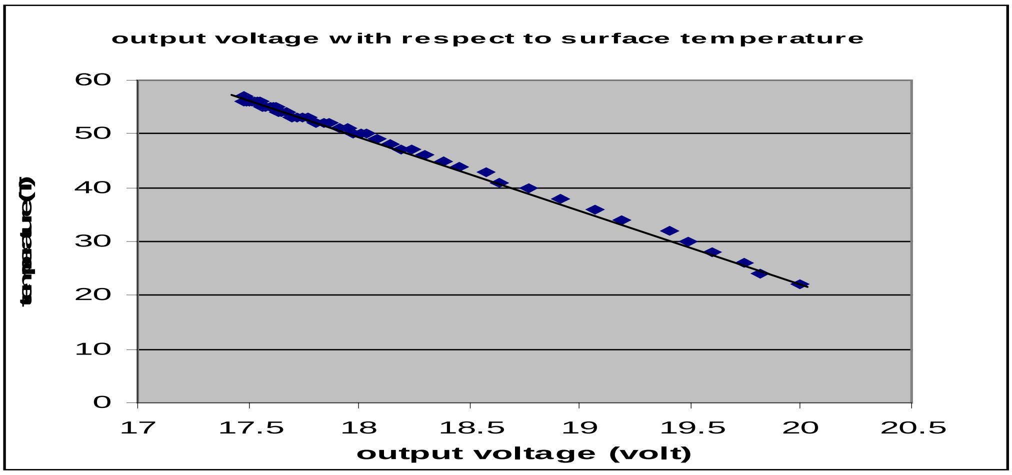

y=mx + c

m=α = (V2-V1)/ (T2-T1) = -0.072

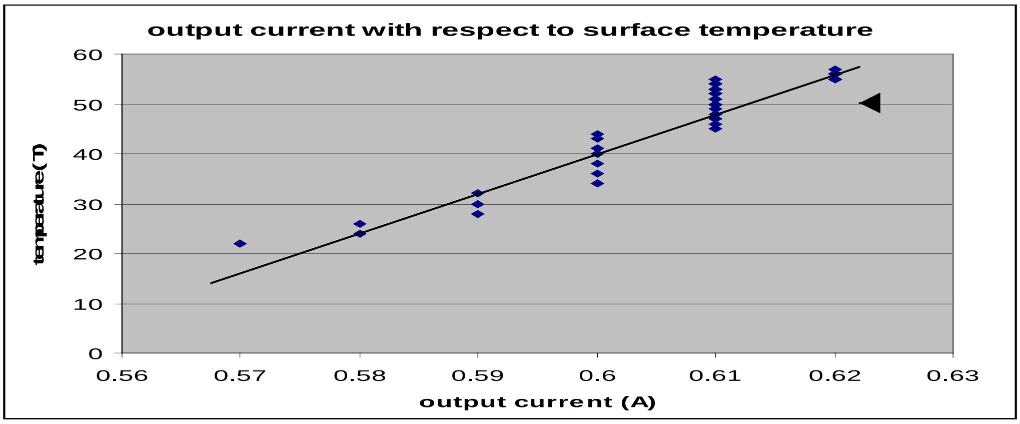

p = m = (I2-I1)/ (T2-T1) = 0.001428

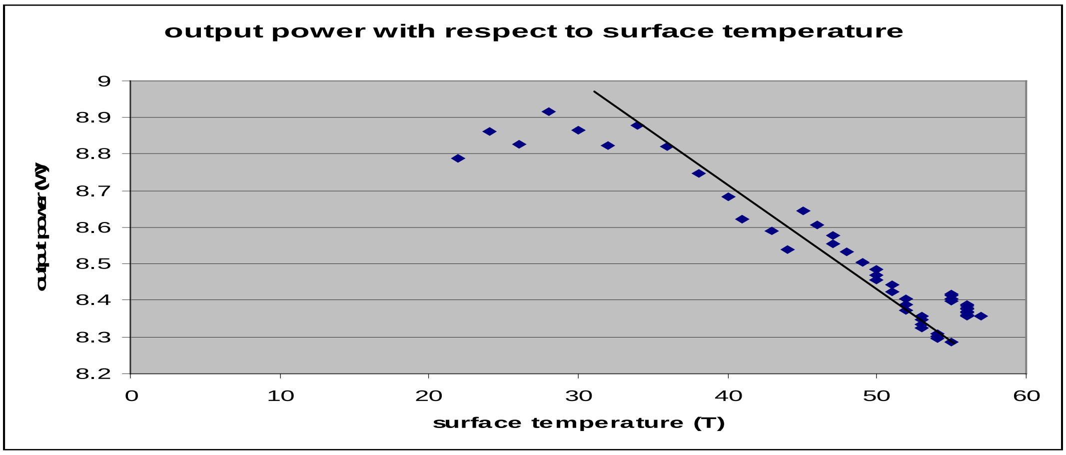

m = (P2-P1)/ (T2-T1) =-0.01239

Figure (5.5) the result for first experiment

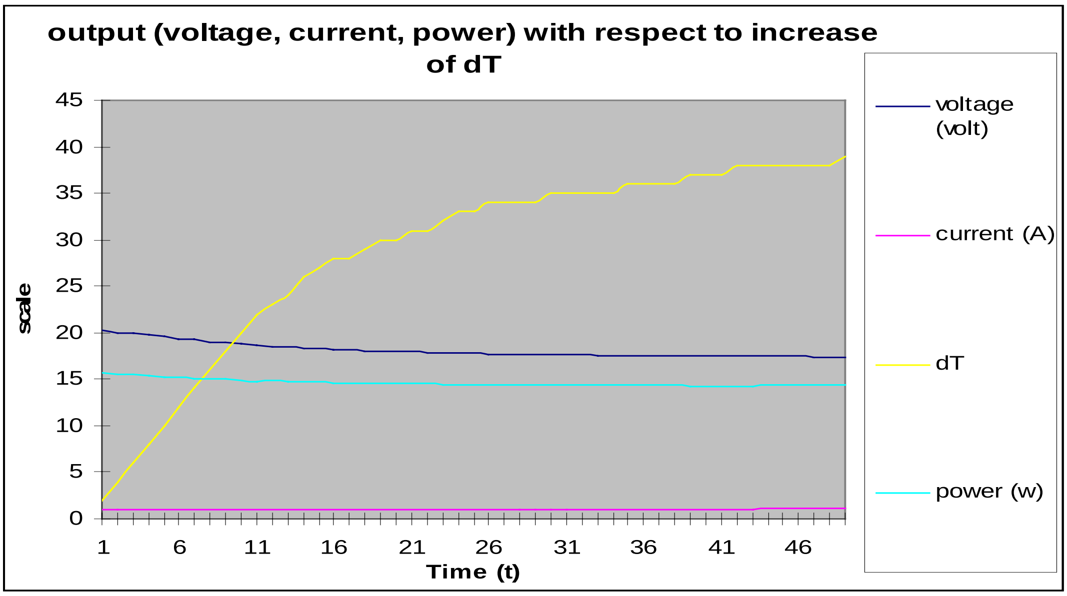
output (voltage, current, power) with respect to increase of dT
scale
45
40
35
30
25
20
15
10
5
0
1
6
11
16
21
26
31
36
41
46
Time (t)
voltage (volt)
current (A)
dT
power (w)

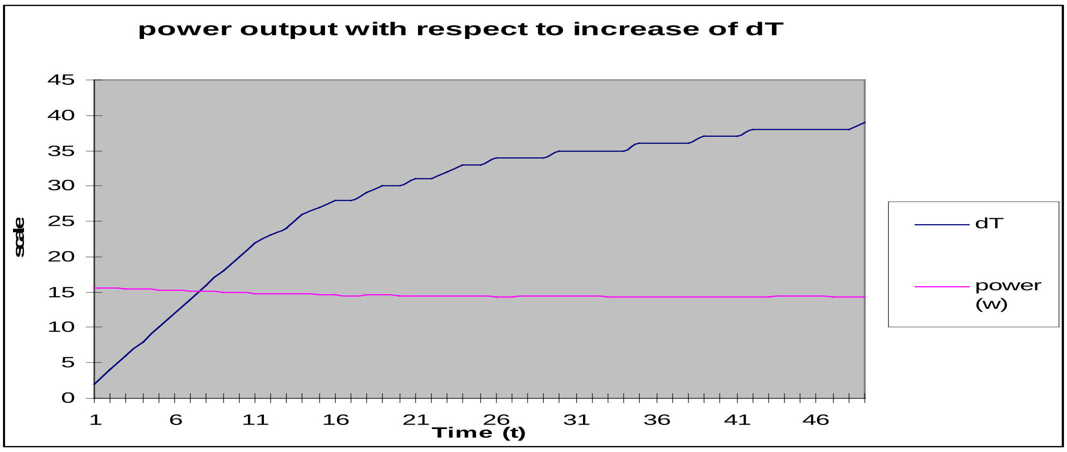
power output with respect to increase of dT
scale
45
40
35
30
25
20
15
10
5
0
1
6
11
16
21
26
31
36
41
46
Time (t)
dT
power (w)

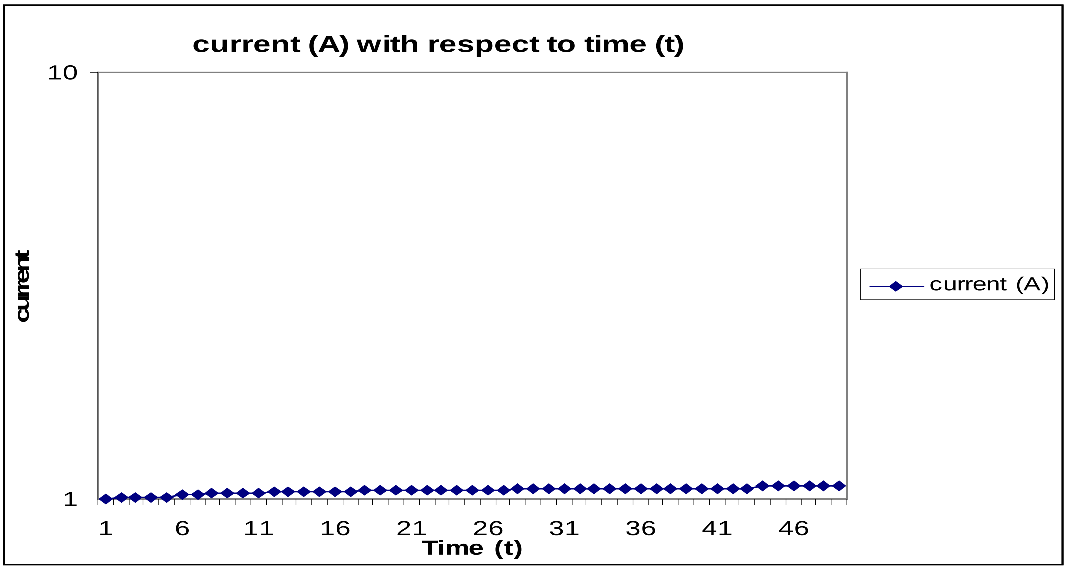
current (A) with respect to time (t)
current
10
1
1
6
11
16
21
26
31
36
41
46
Time (t)
current (A)

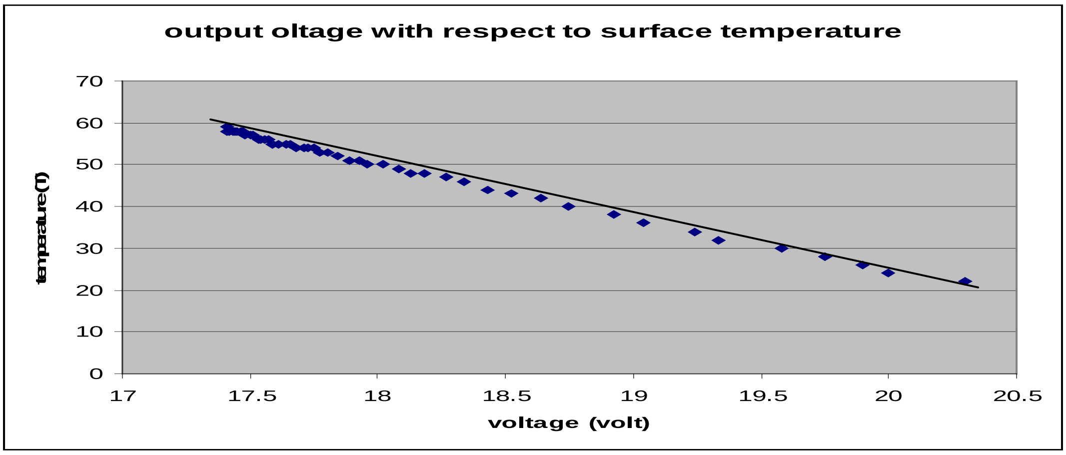

m=α = (V2-V1)/ (T2-T1) = -0.0781

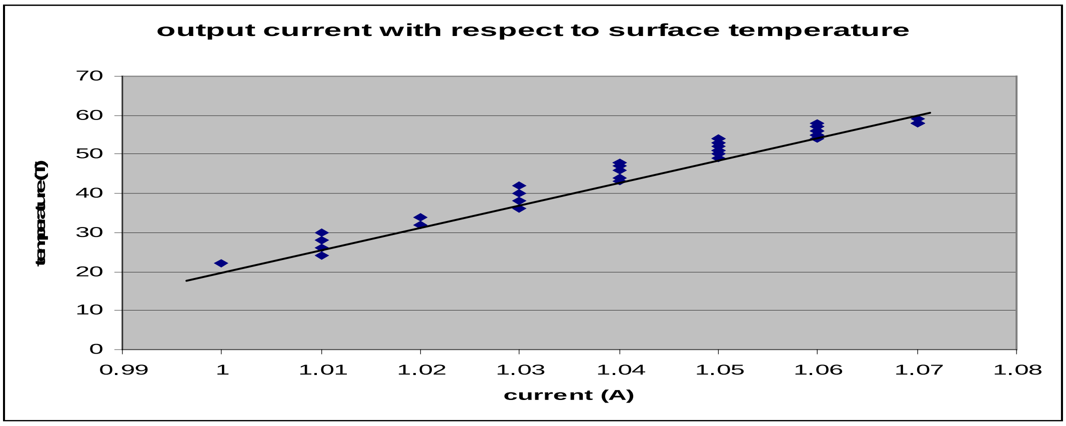

p = m = (I2-I1)/ (T2-T1) = 0.00189

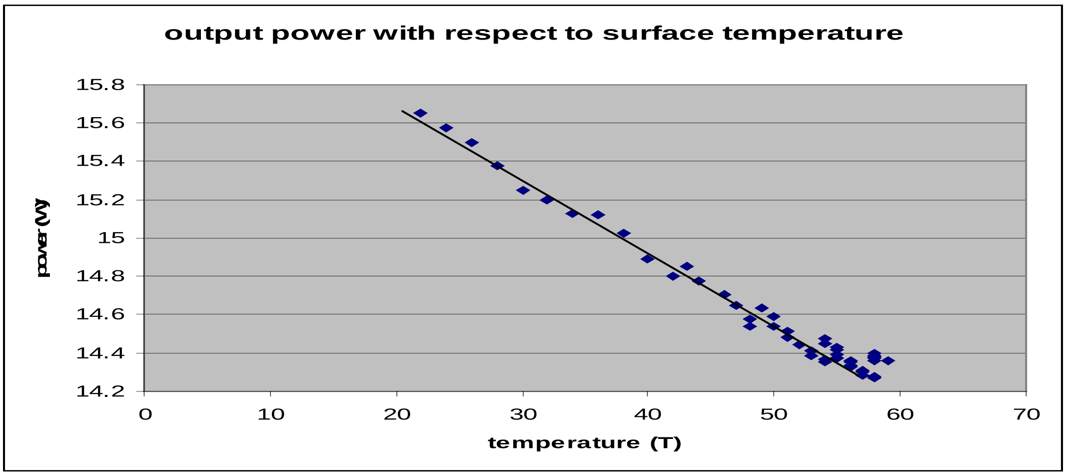

m = (P2-P1)/ (T2-T1) = -0.0348

Figure (5.6) the result for second experiment

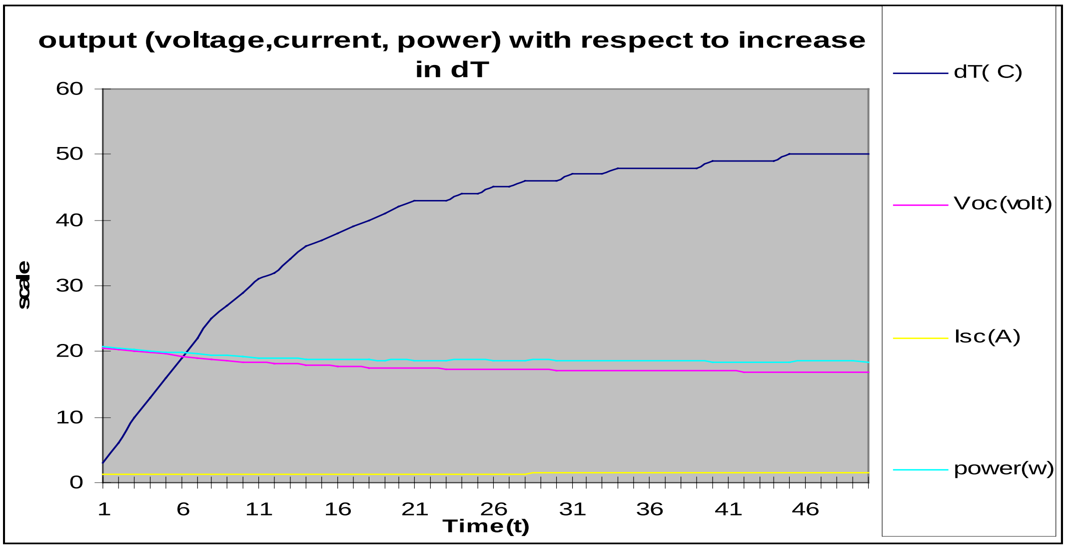
output (voltage,current, power) with respect to increase in dT
scale
Time(t)
dT(C)
Voc(volt)
Isc(A)
power(w)
60
50
40
30
20
10
0
1
6
11
16
21
26
31
36
41
46

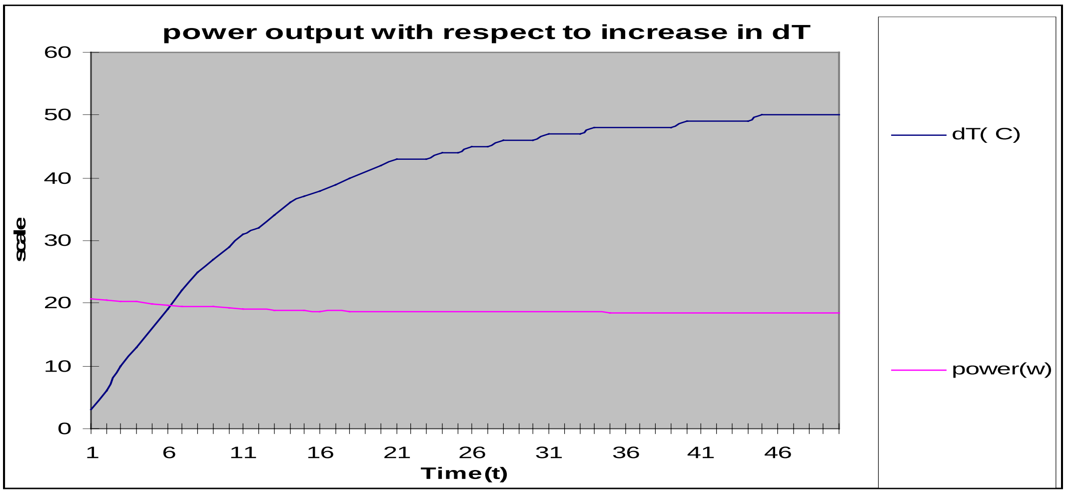
power output with respect to increase in dT
scale
Time(t)
dT(C)
power(w)
60
50
40
30
20
10
0
1
6
11
16
21
26
31
36
41
46

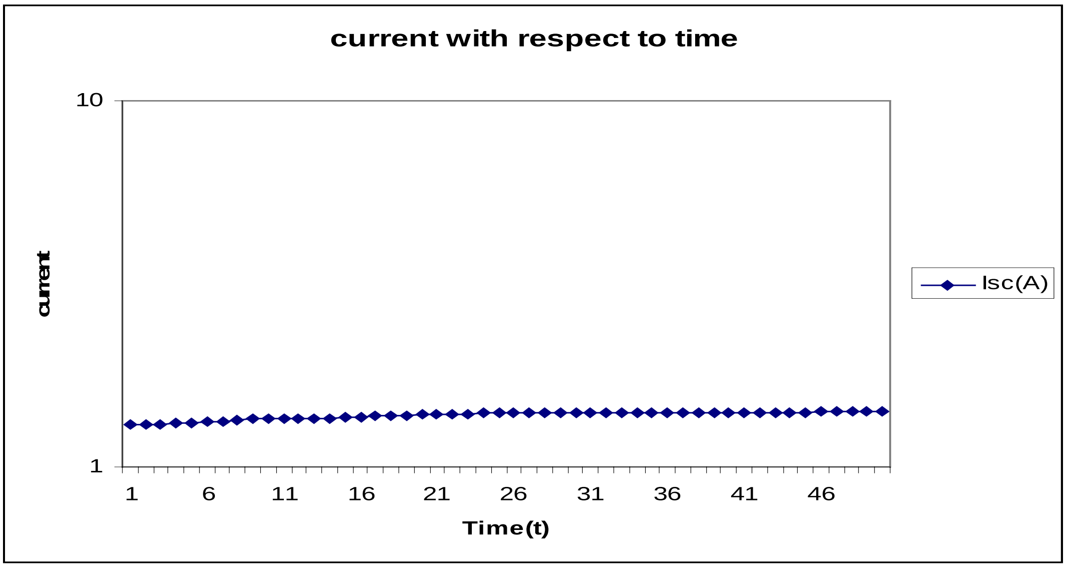
current with respect to time
current
Time(t)
Isc(A)
10
1
1
6
11
16
21
26
31
36
41
46

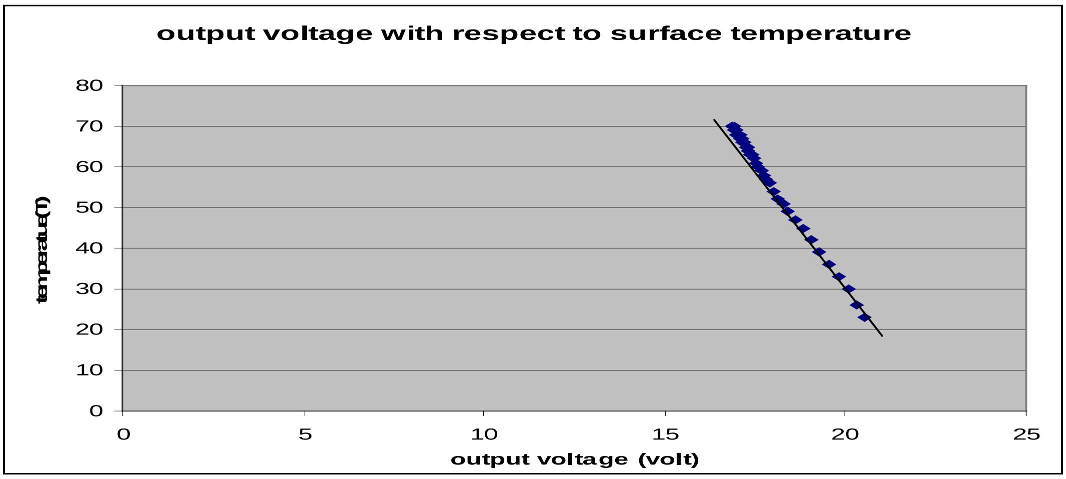

m=α = (V2-V1)/ (T2-T1) = -0.07766

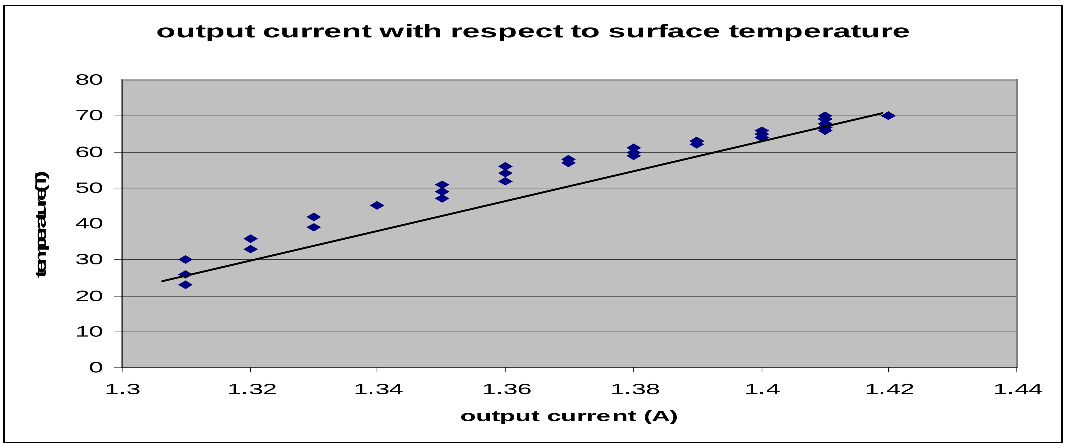

p = m = (I2-I1)/ (T2-T1) = 0.00234

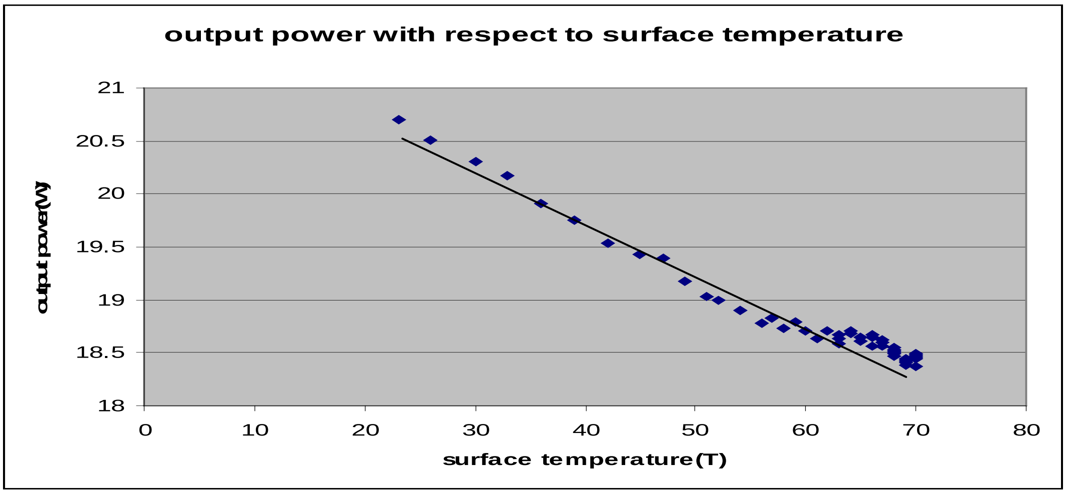

m = (P2-P1)/ (T2-T1) = -0.048

Figure (5.7) the result for third experiment

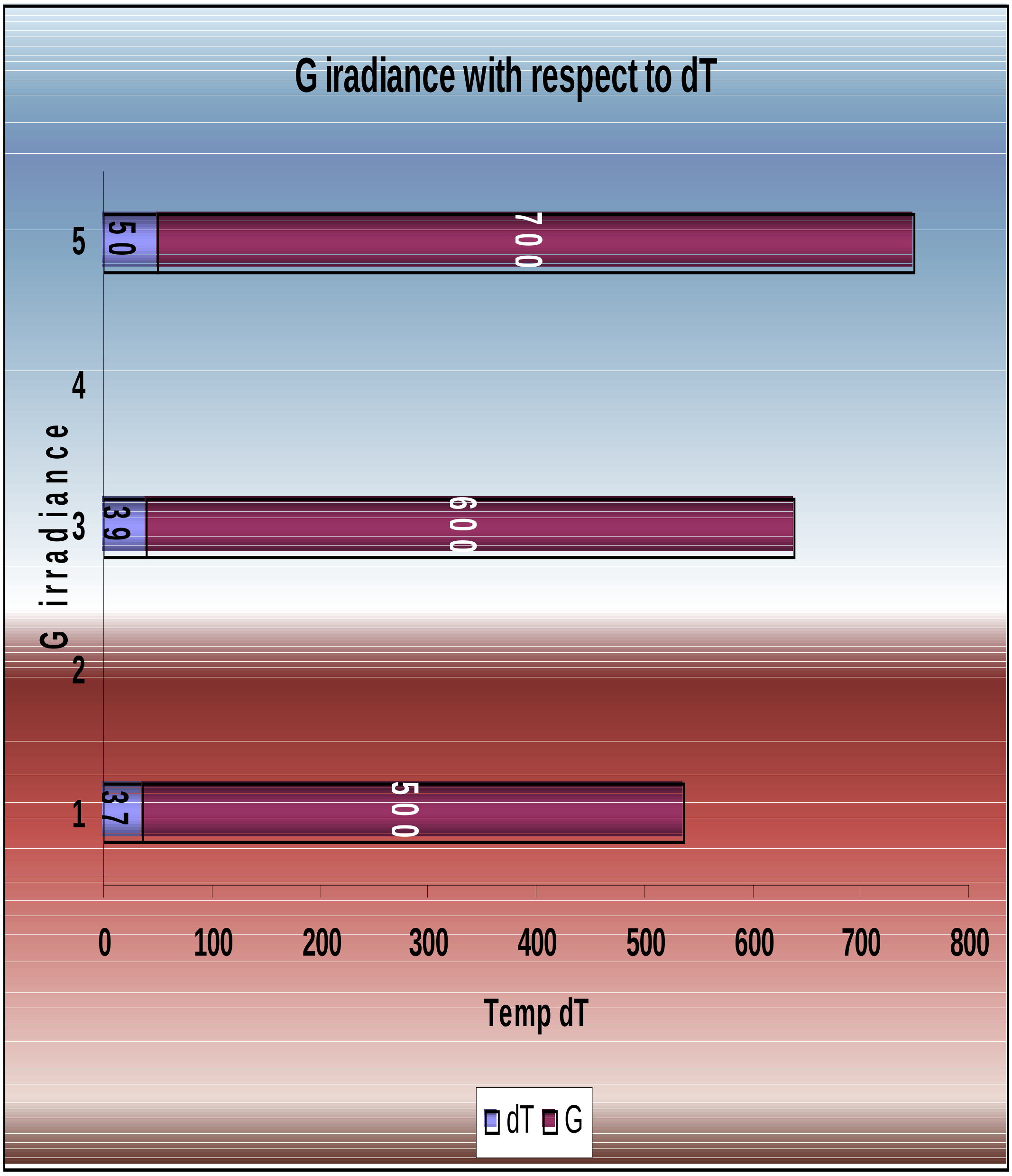

Figure (5.8) maximum ΔT per G irradiance

Discussion

The figures showed the output of current, voltage, power and temperature of the cell surface in respect to the time.

According to the figure (5.5) over the 50 minutes the voltages showed gradual decreased while. The current remained stable but the temperature of the cell surface showed dramatically increased within first 20 minutes, followed by a slight increase thereafter the power output showed a slight decline over the 50 minutes from 1^{st} to 50^{th} minutes. This means that an increase in the cell surface temperature does not have a significant effect on the power output.

The figure (5.6) and figure (5.7) showed that the result of the second experiment was approximately similar to the result of the first experiment, except that the increasing input irradiation has affected on the power output.

Over the test period the power output fell from 8.7 W to 8.3 W for 1st experiment, 2nd experiment from 15.6 W to 14.3 W and for 3rd experiment from 20.7 W to 18.4 W which represents more reduction in 3rd experiment.

There is relationship between ΔT to irradiance G.

For Libya G ≈ 700 W/m^2

Therefore max ΔT at 700 W/m^2

Module temperature in Libya =

= Ambient air temp + max ΔT = 45 + 50 = 95 °C

Specify module power output at 700 W/m^2 and 95 °C.

Therefore the power output for 85Wp module operating in Libya.

G ≈ 700 W/m^2

T module = 95 °C

P_G = (700/1000) * 85 = 59.5 w

M = 0.048 w/°C

Temperature effect = 95 – 25 = 70 °C

Power loss with temperature = 70 * 0.048 = 3.36 w

Then the power for module operating in Libya is 56.1 W about 66% of rated power.

CONCLUSION

A PV module is an electricity generator and requires additional equipment if it is to provide a useful service.

A PV is in the midst of benign cycles where increased sales lead to larger scale production, which leads to lower costs which leads to increased sales. The targets for low-cost production can be met almost entirely by this increasing scale of production, which follows from increased sales. Technological improvements in the solar cells are an additional bonus, although much remains to be done in bringing laboratory-scale performance to commercial production.

Photovoltaics have the potential to become a major electricity generation technology in the next few decades. It will fulfil this potential only if it is recognised that technical success with cells or modules is a necessary but not sufficient criterion for commercial success. It is the PV system that provides the services for which users will pay and these must be designed and implemented to the same level of quality and performance as the modules themselves.

The experiments showed that the power output exhibited a slight decrease as the ΔT value increased. That means there was significant effect of the increasing in the surface temperature on the power output.

There is relationship between temperature ΔT to irradiance G. Therefore in Libya (my country) in which the air temperature reaches 45 °c in summer would result in a maximum surface temperature 95 °c. This increase in temperature together with the lower intensities of irradiance experienced in practice would result in the module tested delivering 66% of its rated power when used in Libya.

REFERENCE:

- Aberle A. G.,Heiser G. and Green M. A. (1994), ‘Two-dimensioal minority carrier flow in high-efficiency silicon solar cells at short-circuit, open-circuit and maximum power point operating conditions’, *Solar Energy Mater. Solar Cells* 34,149-160.

- Brandhorst H. W. and Bernatowicz D. T. (1980), ‘Space solar cells-high efficiency and radiation damage’, Conf. Record 14th. IEEE Photovoltaic Specialists Conf., San Diego, IEEE Press, Piscataway, 667-671.

- Bruton T. M., Luthardt G., Rasch K.-D., Roy K., Dorrity I. A., Garrard B., Teale L., Alonso J., Ugalde U., Declerq K., Nijs J., Szlufcik J., Rauber A., Wettling W. and Vallera A. (1997), ‘A study of the manufacture at 500 MWp p.a. of crystalline silicon photovoltaic modules’, *Proc. 14th. European Photovoltaic Solar Energy* Barcelona, H. S. Stephens & Associates, Bedford, 11-16.

- Eader W. and Swanson R. (1985), ‘Calculation of surface generation and recombination velocities at the Si-Sio_2 interface’, *J.Appl.Phys.* 58, 4267-4276.

- Endros A. L., Einzinger R. and Martinelli, G. (1997), ‘Tri-silicon: a novel substrate for thin wafer solar cells’, *Proc. 14th. European Photovoltaic Solar Energy Conf*., Barcelona, H. S. Stephens & Associates, Bedford, 112-114.

- Ferrazza F. (1996), ‘Growth and post-growth processes of multicrystalline silicon for photovoltaic use’, *in Polycrystalline Semiconductors IV-Physics, Chemistry and Technology,* Pizzini S., Strunk H. P. and Werner J. H., eds., Vol. 51-52, *Solid State Phenomena*, Scitech Publ., Zug, Switzerland.

- Green M. A. (1995*), Silicon Solar Cells: Advanced Principles & Practice*, Centre for Photovoltaic Devices and Systems, University of New South Wales, Sydney.

- Green M.A. and Hansen J. (1998*), Catalogue of Photovoltaic Drawings*, Photovoltaics Special Research Centre, University of New South Wales, Sydney.

- Haas R. (1998), ‘Financial promotion strategies for residential PV systems-an international survey’ *Proc. 2nd. World Conf. Photovoltaic solar Energy Conversion*, Vienna, Joint Research Centre of the European Commission, EUR18656EN, 3333-3338.

- Hebling C., Gaffke R.,Sterk S. and Warta W. (1995), ‘Interdigitated grid for silicon thin-film solar cells on SiO_2 layers’*, Proc. 13th. European Photovoltaic Solar Energy Conf.,* Nice, H. S. Stephens & Associates, Bedford, 1512-1515.

- Hovel H. J. (1975), ‘Solar cells’, Ch. 2 in *Semiconductors and Semimetals*, Vol. 11, Willardson R. K. and Beer A. C., eds., Academic Press, New York.

- Janoch R., Wallace R. and Hanoka J. I. (1997), ‘Commercialization of silicon sheet via the string ribbon crystal growth technique’, Conf. Record 26th. IEEE Photovoltaic Specialists Conf., Anaheim, IEEE Press, Piscataway, 95-98.

- Jorgensen A. M., Clausen T. and Leistiko O. (1997), ‘Novel light trapping scheme for thin crystalline cells utilizing deep structures on both wafer sides’, *Conf. Record 26th. IEEE Photovoltaic Specialists Conf*., Anaheim, IEEE Press, Piscataway, 175-178.

- Kuhlmann B., Aberle A. G. and Hezel R. (1997), ‘Characterization and optimization of the Al/SiO_x/p-Si MIS contact in MIS-IL silicon solar cells’*, Conf. Record 26th. IEEE Photovoltaic Specialists Conf.,* Anaheim, IEEE Press, Piscataway, 79-82.

- Lepley T. (1990), 'Results from the Arizona Public Service Company's STAR Center', *Conf. Record 21st. IEEE Photovoltaic Solar Energy Conf*., Kissimmee, IEEE Press, Piscataway, 903-908.

- Lioret A., Aceves O., Andreu J., Merten J., Puigdollers J., Chantant M., Eicker U. and Sabata L. (1997), 'Lessons learned in the electrical system design, installation and operation of the Mataro Public Library', *Proc. 14th. European Photovoltaic Solar Energy Conf.*, Barcelona, Spain, H. S. Stephens & Associates, Bedford, 1659-1664.

- Lioyd Jones D., Matson C. and Pearsall N. M. (1998), 'The solar office: a solar-powered building with a comprehensive energy strategy', *Proc. 2nd. World Conf. Photovoltaic Solar Energy Conversion*, Vienna, Joint Research Centre of the European Commission, EUR18656EN, 2559-2562.

- Lorenzo E. and Narvarte L. (2000), 'on the usefulness of stand-alone PV sizing methods-the case of SHSs', *Prog. In Photovoltaics*, to be published.

- Maeda Y. and Hide I. (1987), 'Solar cells using spinning Si polycrystale', *Tech. Digest, 3rd. Int. Photovoltaic Sci. Eng. Conf*., 87-92.

- Metz A., Meyer R., Kuhlmann B., Grauvogl M. and Hezel R. (1997), '18.5% efficient first generation MIS inversion-layer silicon solar cells', *Conf. Record 26th. IEEE Photovoltaic Specialists Conf*., Anaheim, IEEE Press, Piscataway, 31-34.

- Nijs J., Demesmaeker E., Szlufcik J., Poortmans J., Frisson L., De Clercq K., Ghannam M., Mertens R. and Van Overstraeten R. (1996), 'Recent improvements in the screen-printing technology and comparison with the buried contact technology by 2D-simulation', *Solar Energy Mater. Solar Cells* 41-42, 101-117.

- Reise C. and Kovach A. (1995), 'PV shading analysis in complex building geometries', *Proc. 13th. European Photovoltaic Solar Energy Conf*., Nice, H. S. Stephens & Associates, Bedford, 2157-2160.

- Shirasawa K., Takahashi H., Inomata Y., Fukui K., Okada M., Takayama M. and Watanabe H. (1994), ‘Large-area high-efficiency multicrystalline silicon solar cells’, *Proc. 12th. European Photovoltaic Solar Energy Conf.,* Amsterdam, H. S. Stephens & Associates, Bedford, 757-760.

- Tiedje T., Yablonovitch E. and Cody G. (1984), ‘Limiting efficiency of silicon solar cells’, *IEEE Trans. Electron Devices* 31, 711-716.

- Verlinden P. J., Sinton R. A., Wickham K., Crane R. A. and Swanson R. M. (1997), ‘Backside-contact silicon solar cells with improved efficiency for the ’96 world solar challenge’, *Proc. 14th. European Photovoltaic Solar Energy Conf*., Barcelona, H. S. Stephens & Associates, Bedford, 96-99.

- Wenham R. (1993), ‘Buried-contact silicon solar cells’, Progress in Photovoltaics 1, 3-10.